nature medicine

CD8$^+$ effector T cells contribute to macrophage recruitment and adipose tissue inflammation in obesity

Satoshi Nishimura[1–4], Ichiro Manabe[1,2,4,5], Mika Nagasaki[1,6], Koji Eto[7], Hiroshi Yamashita[1], Mitsuru Ohsugi[8], Makoto Otsu[7], Kazuo Hara[8], Kohjiro Ueki[3,5,8], Seiryo Sugiura[9], Kotaro Yoshimura[10], Takashi Kadowaki[3,5,8] & Ryozo Nagai[1,3,5]

Inflammation is increasingly regarded as a key process underlying metabolic diseases in obese individuals. In particular, obese adipose tissue shows features characteristic of active local inflammation. At present, however, little is known about the sequence of events that comprises the inflammatory cascade or the mechanism by which inflammation develops. We found that large numbers of CD8$^+$ effector T cells infiltrated obese epididymal adipose tissue in mice fed a high-fat diet, whereas the numbers of CD4$^+$ helper and regulatory T cells were diminished. The infiltration by CD8$^+$ T cells preceded the accumulation of macrophages, and immunological and genetic depletion of CD8$^+$ T cells lowered macrophage infiltration and adipose tissue inflammation and ameliorated systemic insulin resistance. Conversely, adoptive transfer of CD8$^+$ T cells to CD8-deficient mice aggravated adipose inflammation. Coculture and other *in vitro* experiments revealed a vicious cycle of interactions between CD8$^+$ T cells, macrophages and adipose tissue. Our findings suggest that obese adipose tissue activates CD8$^+$ T cells, which, in turn, promote the recruitment and activation of macrophages in this tissue. These results support the notion that CD8$^+$ T cells have an essential role in the initiation and propagation of adipose inflammation.

Inflammation is now considered to have a pivotal role in the development of metabolic diseases[1]. In particular, obese adipose tissue shows the hallmarks of chronic inflammation[2,3], and the inflammation is thought to alter adipose tissue function, leading to systemic insulin resistance[4]. The mechanism by which the development of this insulin resistance occurs is believed to involve proinflammatory cytokines produced by infiltrating macrophages and resident adipocytes within the obese adipose tissue[1]. Likewise, chronic inflammation also impairs triglyceride storage in adipose tissues, and the excess circulating free fatty acids and triglycerides also induces insulin resistance in muscle and liver[5–7]. Adding insult to injury, it has been postulated that a paracrine loop involving these free fatty acids and inflammatory cytokines establishes a vicious cycle that aggravates the inflammatory changes, furthering the dysfunction of adipose tissue[8]. As such, the inflammatory changes seen in obese adipose tissue may be the key pathology that promotes systemic inflammatory states and insulin resistance in obese individuals.

Macrophage infiltration of adipose tissue has been described in both mice and humans[1]. However, little is known about the sequence of events that lead to macrophage infiltration. Recently accumulation of other immune cells, such as T cells, has been documented in obese adipose tissue[9,10]. T lymphocytes are known to interact with macrophages and regulate the inflammatory cascade[11]. However, their functional role in adipose inflammation remains unclear. Here we show that infiltration of CD8$^+$ effector T cells is an early event during the development of adipose tissue obesity induced by a high-fat diet. Further, we show using loss- and gain-of-function approaches *in vivo* that these T cells are critical mediators of systemic metabolic dysfunction. Finally, we also show *in vitro* that obese adipose tissue can activate CD8$^+$ T cells, which, in turn, allows for the recruitment and differentiation of macrophages. Thus, together our findings indicate that CD8$^+$ T cells have essential roles in the initiation and maintenance of adipose tissue inflammation and systemic insulin resistance. Our results also clearly show the involvement of adaptive immunity in metabolic disorders.

RESULTS

CD8$^+$ T cell infiltration precedes macrophage accumulation

Adipose tissue consists of not only adipocytes but also stromal and vascular cells, including fibroblasts, vascular endothelial cells and inflammatory cells. This stromal vascular fraction is known to be essential for adipose tissue inflammation[2]. Therefore, to gain insight

[1]Department of Cardiovascular Medicine, [2]Nano-Bioengineering Education Program and [3]Translational Systems Biology and Medicine Initiative, Graduate School of Medicine, The University of Tokyo, Tokyo, Japan. [4]PRESTO, Japan Science and Technology Agency, Kawaguchi, Japan. [5]Comprehensive Center of Education and Research for Chemical Biology of the Diseases, [6]Computational Diagnostic Radiology and Preventive Medicine, The University of Tokyo, Tokyo, Japan. [7]Division of Stem Cell Therapy, Center for Stem Cell Biology and Regenerative Medicine, Institute of Medical Science, The University of Tokyo, Tokyo, Japan. [8]Department of Metabolic Diseases, Graduate School of Medicine, The University of Tokyo, Tokyo, Japan. [9]Department of Human and Engineered Environmental Studies, Graduate School of Frontier Sciences, The University of Tokyo, Tokyo, Japan. [10]Department of Plastic Surgery, Graduate School of Medicine, The University of Tokyo, Tokyo, Japan. Correspondence should be addressed to S.N. (snishi-tky@umin.ac.jp) or I.M. (manabe-tky@umin.ac.jp).

Received 5 January; accepted 7 April; published online 26 July 2009; doi:10.1038/nm.1964

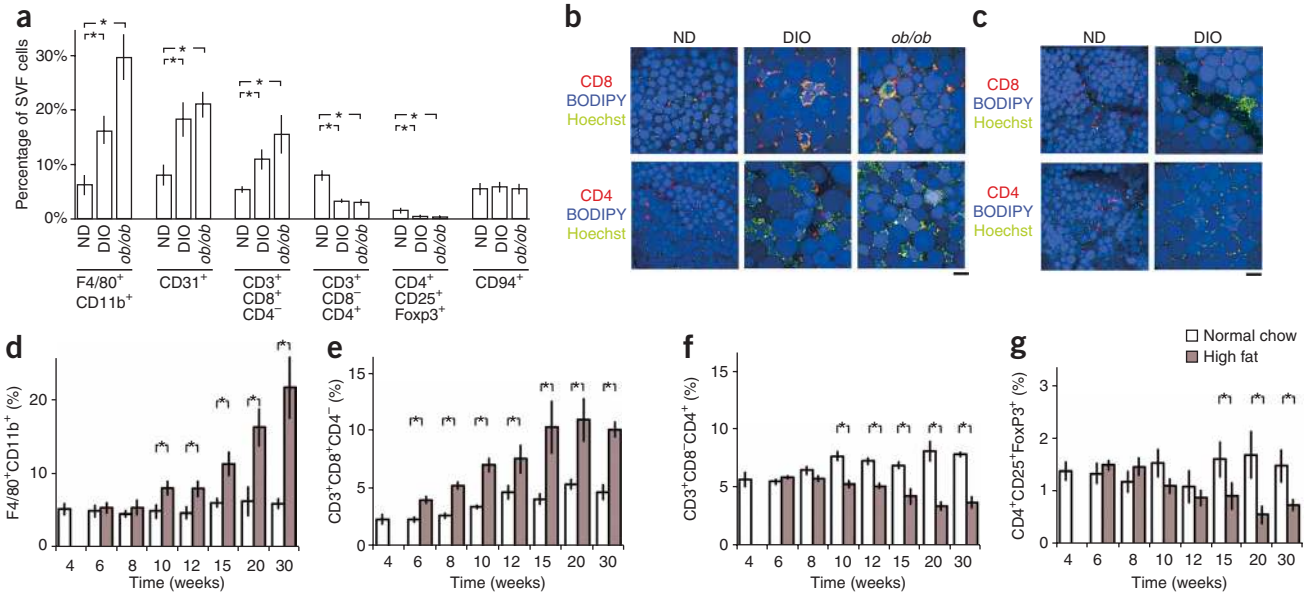

Figure 1 Differential infiltration of lymphocytes and macrophages into obese adipose tissue. (**a**) Flow cytometric analysis of the stromal vascular fraction (SVF) from the epididymal fat pads of control mice fed a normal chow diet (ND), diet-induced obese (DIO) mice fed a high-fat diet for 16 weeks and *ob/ob* mice fed a normal diet (*ob/ob*). All mice were 20-weeks-old. The cell populations of macrophages ($F4/80^+CD11b^+$), endothelial cells ($CD31^+$), $CD3^+CD8^+CD4^-$ T cells, $CD3^+CD8^-CD4^+$ T cells, regulatory T cells ($CD4^+CD25^+Foxp3^+$) and NK cells ($CD3^-CD94^+$) were analyzed ($n = 5$ mice in each group). The number of each cell type was normalized to the total number of viable SVF cells. $^*P < 0.05$. (**b**,**c**) Immunohistochemical analysis of CD8 and CD4 (each in red) in epididymal (**b**) and femoral subcutaneous (**c**) adipose tissue from ND, DIO and *ob/ob* mice. Adipocytes were counterstained with boron-dipyrromethene (BODIPY, blue) and nuclei with Hoechst (green). Quantification of $CD8^+$ and $CD4^+$ cells is shown in **Supplementary Fig. 3**. Scale bars, 100 μm. (**d**–**g**) Time courses of changes in the cell populations in the adipose stroma during development of obesity. Flow cytometric analysis of the stromal vascular fraction from the epididymal fat pads of control mice fed a normal chow diet and mice fed a high-fat diet beginning when they were 4-weeks-old. Numbers of macrophages (**d**), $CD8^+$ T cells (**e**), $CD4^+$ T cells (**f**) and regulatory T cells (**g**) were determined during the course of DIO development ($n = 5$ mice in each group; $^*P < 0.05$). Error bars represent means ± s.e.m.

into the inflammatory processes taking place within these cell fractions during obesity, we first analyzed immune cell populations in collagenase-digested stromal vascular fractions from obese epididymal adipose tissue with the aim of identifying local obesity-induced immunological changes. We acquired stromal vascular fractions using previously described methods of isolation[12] with a few modifications. We first carried out a set of flow cytometric analyses to determine the proper gating for analysis of lymphocytes and macrophages in adipose tissue (**Supplementary Fig. 1**). We found that R1 gating accounted for the majority of viable cells, including a majority of $F4/80^+CD11b^+$ macrophages. Because earlier studies used broader gating to analyze macrophages in the stromal vascular fraction[13], we compared the broader R2 gating with the narrower R1 gating. We found that the macrophage and lymphocyte fractions detected with R1 gating did not significantly differ from those detected using the broader R2 gating (**Supplementary Fig. 1** and **Supplementary Table 1**). For that reason, we analyzed subsequent cell fractions by R1 gating (for further discussion of gating, see **Supplementary Methods** and **Supplementary Fig. 1**).

Consistent with earlier reports[2], the infiltration of $F4/80^+CD11b^+$ macrophages into adipose tissue was significantly increased by diet-induced obesity (DIO) and in obese *ob/ob* mice compared to the control lean mice on a normal diet ($P < 0.05$) (**Fig. 1a**). The numbers of $CD31^+$ endothelial cells were also higher in obese mice (**Fig. 1a**), which may reflect angiogenesis[14]. Notably, we found that $CD3^+$ T cells accounted for 14.8 ± 0.9% of stromal vascular cells in lean adipose tissue, and most (94.7 ± 0.3%) of the $CD3^+$ T cells were CD4 or CD8 positive. The $CD3^+CD8^+CD4^-$ T cell fraction was larger in obese adipose tissue, whereas the $CD3^+CD4^+CD8^-$ T cell fraction was smaller, as was the regulatory T cell fraction ($CD4^+CD25^+Foxp3^+$) compared to lean mice on normal diet ($P < 0.05$). The natural killer (NK) cell fraction ($CD3^-CD94^+$) was unaffected by obesity (**Fig. 1a**). In contrast to the higher number of $CD8^+$ lymphocytes seen in obese adipose tissue, $CD8^+$ and $CD4^+$ T cell counts were significantly lower in peripheral blood from *ob/ob* mice and were unchanged in DIO mice as compared to mice on a normal diet ($P < 0.05$) (**Supplementary Fig. 2**), suggesting selective recruitment of $CD8^+$ T lymphocytes to obese adipose tissues.

Immunohistochemical analysis of F4/80, CD8 and CD4 expression also revealed higher numbers of $F4/80^+$ macrophages and $CD8^+$ T cells and lower numbers of $CD4^+$ T cells in obese epididymal fat pads as compared to mice on a normal diet ($P < 0.05$) (**Fig. 1b** and **Supplementary Fig. 3**). By contrast, we found no significant changes in the numbers of $CD8^+$ and $CD4^+$ cells in subcutaneous fat pads (**Fig. 1c**). In obese epididymal adipose tissues, we found a number of $CD8^+$ cells within 'crown-like structures' (CLSs), which reflect the focal convergence of macrophages surrounding necrotic adipocytes[14,15] (**Fig. 1b**), whereas $CD4^+$ cells showed no apparent relationship with CLSs.

Most $CD3^+CD8^+$ cells were $CD62L^-$ and $CD44^+$ (74.7% ± 3.8% of $CD3^+$ $CD8^+$ cells in DIO mice), suggesting the majority of infiltrated $CD8^+$ T cells were activated effector T cells[16]. To assess the clonality of $CD8^+$ in obese adipose, we examined the T cell receptor (TCR) V_β repertoire of $CD8^+$ T cells in lean and obese adipose tissues. The results showed that $CD8^+$ T cells in obese adipose were not monoclonal, though the $CD8^+$ cell fractions that were positive for $V_{\beta 7}$ and $V_{\beta 20b}$ were significantly larger in obese adipose tissues as compared to mice on a normal diet ($P < 0.05$) (**Supplementary Fig. 4**).

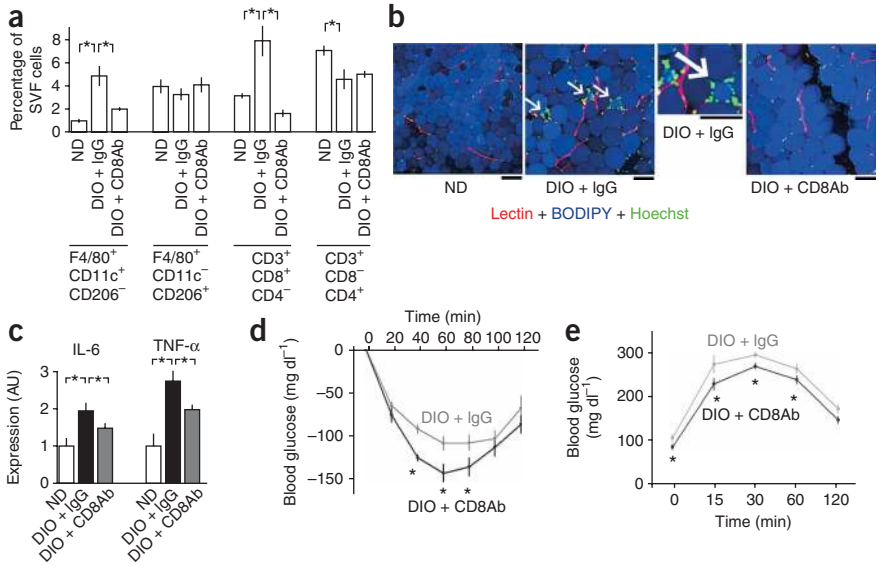

Figure 2 Effects of CD8-specific antibody treatment on obese adipose tissue inflammation. (**a**) Flow cytometric analysis of M1 macrophages ($F4/80^+CD11c^+CD206^-$), M2 macrophages ($F4/80^+CD11c^-CD206^+$), $CD8^+$ T cells and $CD4^+$ T cells in stromal vascular fractions in mice from lean normal-diet (ND), and DIO mice administered either antibody to CD8 (DIO + CD8Ab) or control IgG (DIO + IgG). The same mice were used in **b**–**e**. High-fat diet was started at the age of 4-weeks-old, and all of the mice were examined at 12-weeks-old. ($n = 5$ mice in each group). (**b**) Histochemical identification of endothelial cells (lectin, red), adipocytes (BODIPY, blue) and nuclei (Hoechst, green) in epididymal adipose tissue. White arrows indicate CLSs. Scale bars, 100 μm. (**c**) Real-time PCR analysis of cytokine expression in adipose tissue. The levels of each transcript were normalized to that in the lean control ($n = 5$ mice in each group). AU, arbitrary units. (**d**,**e**) Results of insulin tolerance (**d**, 0.75 U insulin per kg body weight) and oral glucose tolerance (**e**, 1 g per kg glucose) tests in DIO mice treated with antibody to CD8 or control IgG ($n = 8$ mice in each group). $^*P < 0.05$. Error bars represent means ± s.e.m.

It is known that one consequence of macrophage accumulation, particularly M1 macrophages, in inflamed adipose tissue is modulation and impairment of the tissue's function[17]. It is not known, however, what initiates macrophage infiltration or the resultant inflammatory cascade. The dynamic changes in lymphocyte populations seen in obese adipose tissue (**Fig. 1a**,**b**) suggest that lymphocytes might have a key role. To test this idea, we examined the time course of changes in stromal cell populations during the progression of DIO. We fed C57BL/6 mice a high-fat diet, beginning when they were 4-weeks-old (**Fig. 1d**–**g**). Within 2 weeks, the $CD8^+CD4^-$ T cell fraction within the total stromal vascular cell fraction was significantly increased in the stroma of the epididymal fat, as compared to that in mice fed a control chow diet (**Fig. 1e**). The numbers of $CD8^+CD4^-$ T cells continued to increase thereafter, peaking when the mice were 15-weeks-old (**Fig. 1e**). By contrast, the fractions of $CD8^-CD4^+$ T cells and $CD4^+CD25^+FoxP3^+$ regulatory T cells were reduced at later times (**Fig. 1f**,**g**), suggesting that $CD8^+$ T cell infiltration is a primary event during inflammatory cascades within adipose tissue. The increase in $CD8^+$ T cells also preceded the accumulation of macrophages when cell numbers were expressed per fat pad (**Supplementary Fig. 5**), clearly indicating that $CD8^+$ cells infiltrated into the epididymal fat pads of DIO mice before macrophage infiltration.

To gain additional insight into the clinical importance of $CD8^+$ T cells in obese fat, we analyzed the expression of *CD8A* in samples of human subcutaneous adipose tissue. Levels of *CD8A* expression were significantly higher in obese subjects than in lean ones ($P < 0.05$), suggesting that $CD8^+$ T cells also accumulate in human obese adipose tissue (**Supplementary Fig. 6**).

CD8 depletion inhibits inflammatory cascade in obese adipose

To assess the role of $CD8^+$ T cells in adipose inflammation, we examined the effects of CD8 depletion using neutralizing antibody treatment on the inflammatory response in obese adipose tissue. We randomly assigned male C57BL/6 mice to two groups and intraperitoneally administered either antibody to CD8 or control IgG once a week for 8 weeks, beginning when the mice were 4-weeks-old. We fed the mice a high-fat diet over the same period, and we performed metabolic and histological analyses at 12 weeks of age. Antibody to CD8 treatment had no effect on body weight, food intake, fat pad weight or adipocyte diameter (**Supplementary Fig. 7**). However, it significantly lowered the $CD8^+CD4^-$ T cell fraction in the epididymal fat pads without affecting the $CD8^-CD4^+$ cell fraction (**Fig. 2a**). It also reduced the infiltrated M1 macrophage ($F4/80^+CD11c^+CD206^-$) fraction without affecting the M2 macrophage ($F4/80^+CD11c^-CD206^+$) fraction[17] and significantly lowered the numbers of CLSs ($P < 0.05$ for each) (**Fig. 2b** and **Supplementary Fig. 7d**).

The messenger RNA expression of the proinflammatory cytokines interleukin-6 (IL-6) and tumor necrosis factor-α (TNF-α) in epididymal fat pads was lowered by CD8-specific antibody treatment (**Fig. 2c**), as were their serum concentrations (**Supplementary Fig. 7f**). In addition, the insulin resistance and glucose intolerance induced by the high-fat diet were ameliorated by CD8-specific antibody treatment (**Fig. 2d**,**e**). Similarly, CD8-specific antibody treatment lowered M1 macrophage infiltration into epididymal fat and ameliorated systemic insulin resistance in *ob/ob* mice (**Supplementary Fig. 8**). Collectively, these effects of CD8-specific antibody treatment clearly show that $CD8^+$ cells are required for the recruitment of macrophages into obese adipose tissue and the initiation and propagation of inflammatory responses there.

CD8 depletion ameliorates pre-established inflammation

We next examined the activity of $CD8^+$ T cells in obese adipose tissues in which inflammation had already been established. We began administering antibodies to 19-week-old DIO mice that had been fed a high-fat diet since they were 9-weeks-old. We intraperitoneally administered either antibody to CD8 or control IgG three times per week for 2 weeks, and examined the mice at 21-weeks-old. Treatment with antibody to CD8 suppressed $CD8^+$ T cell infiltration into obese fat pads without affecting $CD4^+$ T cells (**Fig. 3a**). CD8 antibody also lowered M1 ($F4/80^+CD11c^+$) macrophage fraction while leaving the M2 macrophage ($F4/80^+CD11c^-$) fraction unchanged (**Fig. 3a**). The reduction in macrophage infiltration was confirmed by F4/80 immunohistochemistry (**Fig. 3b**). In addition, the number of CLSs was also lowered by CD8-specific antibody treatment (**Fig. 3b**,**c**). DIO led to upregulated mRNA expression of the proinflammatory cytokines IL-1, IL-6 and TNF-α, as well as of

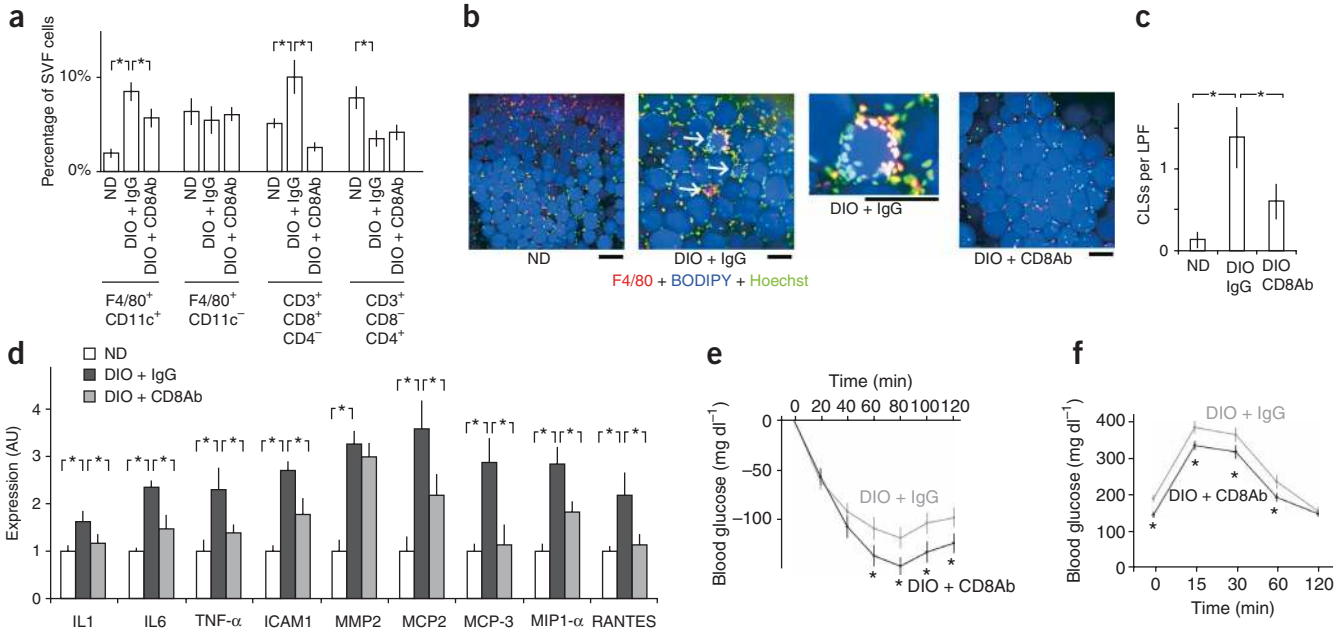

Figure 3 Effects of CD8-specific antibody treatment on pre-established obese adipose inflammation. (**a**) Flow cytometric analysis of cell populations in stromal vascular fractions from control mice on a normal chow diet (ND) and DIO mice administered control IgG (DIO + IgG) or antibody to CD8 (DIO + CD8Ab) three times per week from 19- to 21-weeks-old. ($n = 5$ mice in each group). High-fat diet was started at the age of 9-weeks-old, and all the mice were examined at 21-weeks-old. The same mice were used in **b**–**f**. (**b**) Immunohistochemical identification of macrophages (F4/80, red) in epididymal adipose tissue. Adipocytes were counterstained with BODIPY (blue), and the nuclei with Hoechst (green). Scale bars, 100 μm. (**c**) Numbers of CLSs (shown by white arrows in **b**) in adipose tissue ($n = 20$ low-power fields (LPF) in each group). (**d**) Real-time PCR analysis of cytokine expression in epididymal adipose tissue. The levels of each transcript were normalized to those in control ND mice. MIP, monocyte inflammatory protein ($n = 5$ mice in each group). (**e**,**f**) Results of insulin tolerance (**e**, 1 U insulin per kg body weight) and oral glucose tolerance (**f**, 1 g per kg glucose) tests in DIO mice treated with antibody to CD8 or control IgG ($n = 10$ mice in each group). $^*P < 0.05$. Error bars represent means ± s.e.m.

intercellular adhesion molecule-1 (ICAM1) and matrix metalloproteinase-2 (MMP-2), in adipose tissue, which is consistent with local inflammation, and CD8-specific antibody treatment lowered expression of all of these mediators (**Fig. 3d**).

CD8-specific antibody treatment also ameliorated insulin resistance and glucose intolerance in DIO mice (**Fig. 3e**,**f** and **Supplementary Fig. 9**). These results clearly show that CD8-specific antibody treatment suppresses preexisting adipose inflammation, which strongly suggests that $CD8^+$ cells are required for the maintenance of inflammatory reactions in obese adipose tissue.

$CD8^+$ T cells are required for adipose tissue inflammation

To further establish the requirement for $CD8^+$ T cells in adipose inflammation *in vivo*, we started 6-week-old genetically CD8-deficient mice on a high-fat diet and maintained them on it for 8 weeks, and examined the $CD8a^{-/-}$ mice at 14-weeks-old. In sharp contrast to wild-type mice fed the same high-fat diet (**Fig. 1**), the CD8-deficient mice did not show significant increases in the M1 or M2 macrophage fraction in the epididymal fat under high-fat diet (**Fig. 4a**), and we found very few CLSs (**Fig. 4b**,**c**), although both body weight and epididymal fat mass were significantly higher compared to $CD8a^{-/-}$ mice on a normal diet (**Supplementary Fig. 10a**,**b**). Levels of proinflammatory cytokine mRNA expression in adipose tissue, including IL-6 and TNF-α, also were not increased by the high-fat diet in CD8-deficient mice (**Fig. 4d**).

To directly examine the role of $CD8^+$ T cells in adipose tissue inflammation, we adoptively transferred splenic $CD8^+$ T cells into CD8-deficient mice. We intravenously administered either 5×10^6 splenic $CD8^+$ T cells isolated from 7-week-old C57BL/6 mice or control vehicle weekly over the same period and examined the $CD8a^{-/-}$ mice at 14-weeks-old. Adoptive transfer of $CD8^+$ T cells increased M1 macrophage infiltration (**Fig. 4a**), numbers of CLSs (**Fig. 4b**,**c**), and expression of IL-6 and TNF-α in epididymal fat (**Fig. 4d**), indicating initiation of adipose inflammation. A high-fat diet induced moderate glucose intolerance in untreated CD8-deficient mice, but we did not observe insulin resistance in insulin tolerance tests (**Fig. 4e**,**f**). Adoptive $CD8^+$ T cell transfer aggravated the glucose intolerance and induced insulin resistance (**Fig. 4e**,**f**). Taken together, the results that we obtained with CD8-deficient mice confirm that $CD8^+$ T cells are essential for macrophage recruitment and inflammation in adipose tissue in DIO.

Interplay between macrophages, T cells and adipocytes

We next analyzed the cellular interplay via which inflammation develops in obese adipose tissue. On the basis of the findings of the *in vivo* experiments summarized above, we hypothesized that obese adipose tissue activates $CD8^+$ T cells, which, in turn, recruit and activate macrophages. To test this hypothesis, we first cocultured splenic $CD8^+$ T cells with epididymal fat tissue prepared from lean or obese mice to determine whether obese adipose tissue can activate $CD8^+$ T cells. Whereas obese epididymal fat clearly induced T cell proliferation, lean fat did so only modestly (**Fig. 5a**), indicating that obese adipose tissue can indeed activate $CD8^+$ T cells.

To assess the involvement of $CD8^+$ T cells in monocytes and macrophage differentiation, we cocultured various combinations of peripheral blood $CD11b^{high}$ granulocyte-1 $(Gr\text{-}1)^-CD4^-CD8^-$cells (most of which were monocytes), $CD8^+$ cells prepared from either lean or obese adipose tissue, and lean epididymal adipose tissue. By

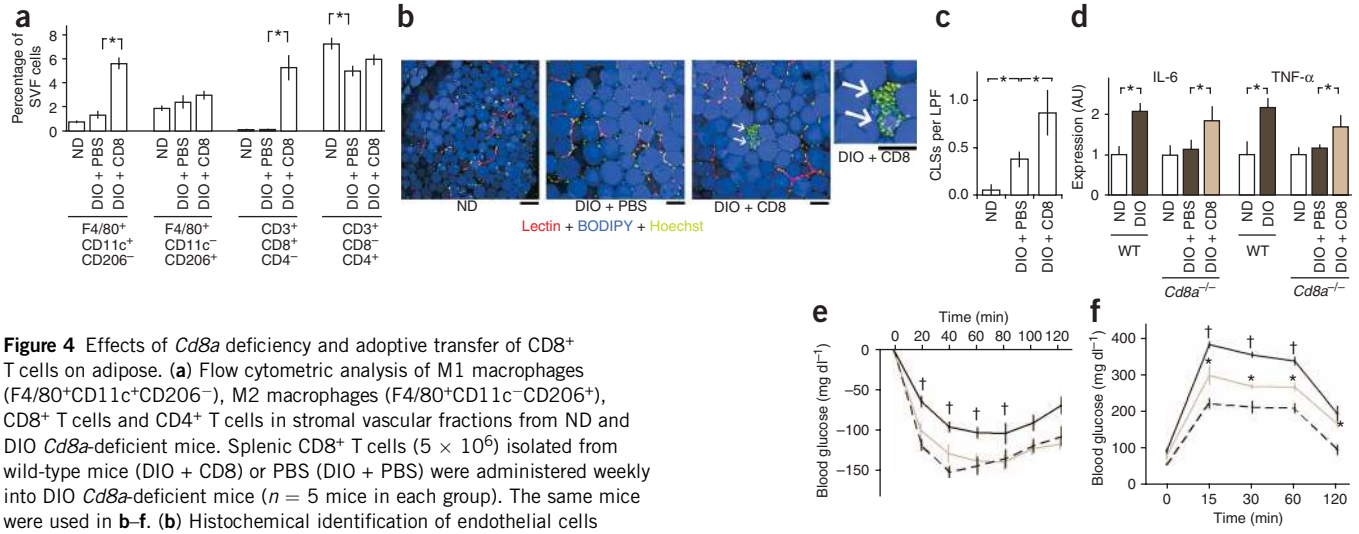

Figure 4 Effects of *Cd8a* deficiency and adoptive transfer of CD8$^+$ T cells on adipose. (**a**) Flow cytometric analysis of M1 macrophages (F4/80$^+$CD11c$^+$CD206$^-$), M2 macrophages (F4/80$^+$CD11c$^-$CD206$^+$), CD8$^+$ T cells and CD4$^+$ T cells in stromal vascular fractions from ND and DIO *Cd8a*-deficient mice. Splenic CD8$^+$ T cells (5×10^6) isolated from wild-type mice (DIO + CD8) or PBS (DIO + PBS) were administered weekly into DIO *Cd8a*-deficient mice ($n = 5$ mice in each group). The same mice were used in **b**–**f**. (**b**) Histochemical identification of endothelial cells (lectin, red), adipocytes (BODIPY, blue) and nuclei (Hoechst, green) in epididymal adipose tissue. White arrows indicate CLSs. Scale bars, 100 μm. (**c**) Numbers of CLSs in adipose tissues ($n = 20$ low-power fields in each group). (**d**) Real-time PCR analysis of cytokine expression in adipose tissue from C57BL/6 (WT) ND, WT DIO, and *Cd8a*-deficient ND, DIO + CD8 or DIO + PBS mice. ($n = 5$ mice in each group). *$P < 0.05$ in **a**–**d**. (**e**,**f**) Insulin tolerance (**e**, 0.75 U insulin per kg body weight) and oral glucose tolerance (**f**, 1 g per kg) tests of the *Cd8a*-deficient ND (dotted lines), DIO + CD8 and DIO + PBS groups ($n = 6$ mice in each group). *$P < 0.05$ for ND versus DIO + PBS and †$P < 0.05$ for DIO + PBS versus DIO + CD8. Error bars represent means ± s.e.m.

themselves, neither CD8$^+$ cells nor adipose tissue induced macrophage differentiation (**Fig. 5b**). However, when cocultured with both CD8$^+$ cells and lean adipose tissue, peripheral blood monocytes differentiated into F4/80$^+$CD11b$^+$CD68$^+$ macrophages (**Fig. 5b**). Moreover, CD8$^+$ cells from obese adipose tissues generated significantly more macrophages than those from lean adipose (**Fig. 5b**). Thus, CD8$^+$ cells seem to be essential for macrophage differentiation in this setting. Further, the requirement for adipose tissue suggests that the interaction between CD8$^+$ T cells and adipose tissue is necessary for induction of macrophage differentiation.

We then tested whether activated CD8$^+$ cells elicit macrophage migration via humoral interactions. Analysis of the medium conditioned with activated CD8$^+$ T cells showed that these cells secrete substantial amounts of humoral factors known to induce macrophage

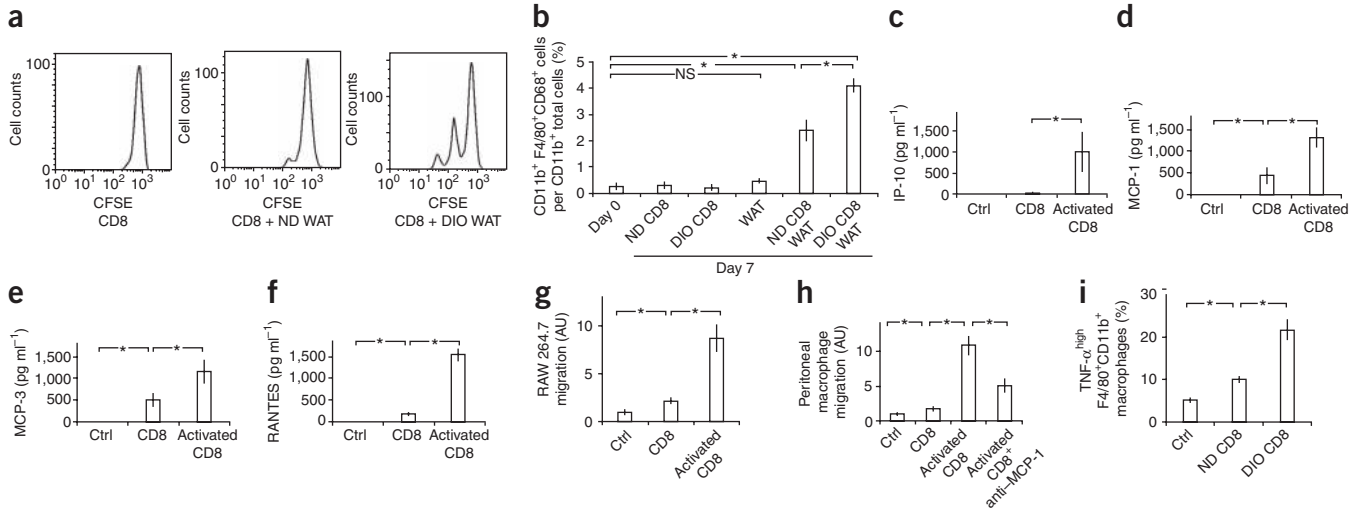

Figure 5 Interplay between macrophages, CD8$^+$ T cells and adipose tissue. (**a**) Carboxyfluorescein succinimidyl ester (CFSE) proliferation assay of isolated splenic CD8$^+$ T cells cultured with or without epididymal adipose tissue from ND or DIO mice. WAT, white adipose tissue. (**b**) Effects of CD8$^+$ T cells and adipose tissue on differentiation of peripheral blood monocytes (CD11b^{high}Gr-1$^-$) into macrophages (CD11b$^+$F4/80$^+$CD68$^+$). Monocytes were cocultured for 7 d with CD8$^+$ T cells isolated from epididymal adipose tissue from lean (ND CD8) or DIO (DIO CD8) mice, with or without epididymal WAT from lean mice. The differentiated macrophage fractions are shown ($n = 5$ in each group; *$P < 0.05$; NS, not significant). (**c**–**f**) Concentrations of various cytokines in the control medium and medium conditioned by quiescent (CD8) or activated (activated CD8) CD8 cells ($n = 5$ in each group). *$P < 0.05$. IP-10, interferon-inducible protein-10. (**g**,**h**) Migration of RAW264.7 (**g**) and peritoneal (**h**) macrophages, as examined using unconditioned control medium (Ctrl), medium conditioned by quiescent (CD8) or activated (activated CD8) CD8$^+$ T cells, or neutralizing antibody to MCP-1 (anti–MCP-1) ($n = 20$ in each group). *$P < 0.05$. (**i**) The fraction of F4/80$^+$ CD11b$^+$ macrophages producing high levels of TNF-α after isolation from lean epididymal adipose tissue and cultured without (Ctrl) or with CD8$^+$ T cells isolated from ND (ND CD8) or DIO (DIO CD8) mice ($n = 5$ in each group, *$P < 0.05$). Error bars represent means ± s.e.m.

migration, including interferon-inducible protein-10, monocyte chemoattractant protein-1 (MCP-1), MCP-3 and regulation upon activation, normal T cell expressed and secreted protein (RANTES) (**Fig. 5c–f**). When we plated cells of the macrophage cell line RAW264.7 or isolated peritoneal macrophages in Boyden chambers and treated them with medium conditioned by activated $CD8^+$ T cells, the numbers of both cell types that migrated through the pores between the chamber wells with activated $CD8^+$ T cell–conditioned medium were significantly higher compared to cells cultured in non-conditioned medium ($P < 0.05$ for each) (**Fig. 5g,h**). Treatment with antibody to MCP-1 lowered the migration of peritoneal macrophages by approximately half, indicating MCP-1 to be one of the factors mediating the humoral interactions (**Fig. 5h**).

To further assess the involvement of $CD8^+$ T cells in macrophage activation in adipose tissue, we cocultured $F4/80^+$ $CD11b^+$ macrophages isolated from lean epididymal fat tissue with $CD8^+$ cells isolated from either lean or obese fat tissue. The numbers of macrophages producing high amounts of TNF-α were significantly increased by the $CD8^+$ cells (**Fig. 5i**). Moreover, $CD8^+$ cells from obese adipose tissue increased the number of TNF-α^{high} macrophages to a significantly greater degree than those from lean adipose tissue (**Fig. 5i**). Collectively, then, the results of the coculture experiments show that the interaction between obese adipose tissue and $CD8^+$ T cells is crucial for macrophage differentiation, migration and activation.

DISCUSSION

Adipose tissue inflammation is now considered to be a crucial event leading to the metabolic syndrome, diabetes and atherosclerotic cardiovascular disease. However, it is still unclear how adipose inflammation is initiated and maintained. Here we showed that $CD8^+$ T cell infiltration precedes accumulation of macrophages in adipose tissue obesity, $CD8^+$ T cells are required for adipose tissue inflammation and $CD8^+$ T cells have major roles in macrophage differentiation, activation and migration. Thus, $CD8^+$ T cells are crucially involved in initiating inflammatory cascades in obese adipose tissue. Moreover, the finding that CD8-specific antibody treatment ameliorates preestablished adipose inflammation in DIO mice indicates that $CD8^+$ T cells are also essential for maintenance of the inflammatory response. Although infiltration of T cells into obese adipose tissue has been reported previously[10,18], to our knowledge, the present study is the first to directly address the functional role of $CD8^+$ cells in adipose tissue inflammation. The findings that systemic insulin resistance is ameliorated by CD8 depletion and aggravated by adoptive transfer of $CD8^+$ cells strongly suggest that CD8-dependent adipose inflammation has an impact on systemic metabolism.

Accumulation of $CD8^+$ T cells in obese epididymal fat pads was not accompanied by the presence of greater numbers of $CD8^+$ T cells in the systemic circulation, suggesting that $CD8^+$ T cells are activated by endogenous stimuli localized in the adipose tissue. Supporting this notion is our finding that obese adipose tissue induces $CD8^+$ T cell proliferation. The findings that incubation with $CD8^+$ T cells plus lean adipose tissue induced macrophage differentiation, although neither $CD8^+$ T cells nor lean adipose tissue did so alone, suggest that $CD8^+$ T cells and adipose tissue interact with each other to activate a local inflammatory cascade. In addition, the results of coculture experiments showing the interactions among $CD8^+$ T cells, macrophages and adipose tissue, as well as the results of our CD8 depletion experiments, which showed that $CD8^+$ T cells are essential for both the initiation and maintenance of adipose inflammation, strongly suggest that there is a relay involving both $CD8^+$ T cells and macrophages in obese adipose tissue that propagates local adipose inflammation.

In contrast to the increased infiltration of $CD8^+$ T cells, numbers of $CD4^+$ T cells and regulatory T cells were low at later time points (**Fig. 1**), which would also be expected to contribute to local inflammation within adipose tissue. For instance, subsets of $CD4^+$ T cells are known to secrete cytokines that can inhibit macrophage recruitment, including IL-4 and IL-10 (ref. 19), whereas regulatory T cells control adaptive immune responses by suppressing T cells, NK cells, NKT cells, B cells and dendritic cells[20]. In addition, regulatory T cells have also been shown to inhibit proinflammatory activation of monocytes[21] and to inhibit macrophage infiltration and renal injury in a model of chronic kidney disease[22]. It is therefore tempting to speculate that reducing the numbers of $CD4^+$ and regulatory T cells augments the inflammatory response during the late phase of adipose tissue obesity.

Taken together, our results support the idea that obese adipose tissue activates $CD8^+$ T cells, which, in turn, initiate and propagate inflammatory cascades, including the recruitment of monocytes and macrophages into obese adipose tissues and their subsequent differentiation and activation there. Thus, it seems that $CD8^+$ T cells have a primary role in obese adipose tissue inflammation, though future studies are needed to address which environmental cues within obese adipose tissue initiate $CD8^+$ cell infiltration. Even so, these results further support the idea that adipose inflammation has a major impact on systemic metabolism.

METHODS

Methods and any associated references are available in the online version of the paper at http://www.nature.com/naturemedicine/.

Note: Supplementary information is available on the Nature Medicine website.

ACKNOWLEDGMENTS

We gratefully acknowledge A. Matsuoka, X. Yingda, E. Magoshi, M. Hayashi, K. Wakabayashi, M. Tajima and Y. Yamazaki for excellent technical assistance. This study was supported by Research Fellowships from the Japan Society for the Promotion of Science for Young Scientists (S.N.), Grants-in-Aid for Scientific Research (I.M., R.N.) and grants for Translational Systems Biology and Medicine Initiative (R.N., T.K.) and Global Centers of Excellence program (R.N., T.K.) from the Ministry of Education, Culture, Sports, Science and Technology of Japan and a research grant from the National Institute of Biomedical Innovation (R.N.).

AUTHOR CONTRIBUTIONS

S.N. and M.N. performed *in vivo* and *in vitro* assays and analyzed all of the end points. K.H., K.U. and K.Y. performed human subject assays. S.N., I.M., K.E., H.Y., M. Otsu, M. Ohsugi, S.S., T.K. and R.N. supervised entire studies. S.N. and I.M. wrote the manuscript.

Published online at http://www.nature.com/naturemedicine/.
Reprints and permissions information is available online at http://npg.nature.com/reprintsandpermissions/.

1. Hotamisligil, G.S. Inflammation and metabolic disorders. *Nature* **444**, 860–867 (2006).
2. Weisberg, S.P. *et al.* Obesity is associated with macrophage accumulation in adipose tissue. *J. Clin. Invest.* **112**, 1796–1808 (2003).
3. Nishimura, S. *et al. In vivo* imaging in mice reveals local cell dynamics and inflammation in obese adipose tissue. *J. Clin. Invest.* **118**, 710–721 (2008).
4. Xu, H. *et al.* Chronic inflammation in fat plays a crucial role in the development of obesity-related insulin resistance. *J. Clin. Invest.* **112**, 1821–1830 (2003).
5. Savage, D.B., Petersen, K.F. & Shulman, G.I. Disordered lipid metabolism and the pathogenesis of insulin resistance. *Physiol. Rev.* **87**, 507–520 (2007).
6. Guilherme, A., Virbasius, J.V., Puri, V. & Czech, M.P. Adipocyte dysfunctions linking obesity to insulin resistance and type 2 diabetes. *Nat. Rev. Mol. Cell Biol.* **9**, 367–377 (2008).
7. Shoelson, S.E., Lee, J. & Goldfine, A.B. Inflammation and insulin resistance. *J. Clin. Invest.* **116**, 1793–1801 (2006).
8. Suganami, T., Nishida, J. & Ogawa, Y. A paracrine loop between adipocytes and macrophages aggravates inflammatory changes: role of free fatty acids and tumor necrosis factor alpha. *Arterioscler. Thromb. Vasc. Biol.* **25**, 2062–2068 (2005).

9. Wu, H. *et al.* T-cell accumulation and regulated on activation, normal T cell expressed and secreted upregulation in adipose tissue in obesity. *Circulation* **115**, 1029–1038 (2007).
10. Rausch, M.E., Weisberg, S., Vardhana, P. & Tortoriello, D.V. Obesity in C57BL/6J mice is characterized by adipose tissue hypoxia and cytotoxic T-cell infiltration. *Int. J. Obes. (Lond.)* **32**, 451–463 (2008).
11. Monney, L. *et al.* T_H1-specific cell surface protein Tim-3 regulates macrophage activation and severity of an autoimmune disease. *Nature* **415**, 536–541 (2002).
12. Brake, D.K., Smith, E.O., Mersmann, H., Smith, C.W. & Robker, R.L. ICAM-1 expression in adipose tissue: effects of diet-induced obesity in mice. *Am. J. Physiol. Cell Physiol.* **291**, C1232–C1239 (2006).
13. Traktuev, D.O. *et al.* A population of multipotent CD34-positive adipose stromal cells share pericyte and mesenchymal surface markers, reside in a periendothelial location and stabilize endothelial networks. *Circ. Res.* **102**, 77–85 (2008).
14. Nishimura, S. *et al.* Adipogenesis in obesity requires close interplay between differentiating adipocytes, stromal cells and blood vessels. *Diabetes* **56**, 1517–1526 (2007).
15. Cinti, S. *et al.* Adipocyte death defines macrophage localization and function in adipose tissue of obese mice and humans. *J. Lipid Res.* **46**, 2347–2355 (2005).
16. Sallusto, F., Lenig, D., Forster, R., Lipp, M. & Lanzavecchia, A. Two subsets of memory T lymphocytes with distinct homing potentials and effector functions. *Nature* **401**, 708–712 (1999).
17. Lumeng, C.N., Bodzin, J.L. & Saltiel, A.R. Obesity induces a phenotypic switch in adipose tissue macrophage polarization. *J. Clin. Invest.* **117**, 175–184 (2007).
18. Kintscher, U. *et al.* T-lymphocyte infiltration in visceral adipose tissue: a primary event in adipose tissue inflammation and the development of obesity-mediated insulin resistance. *Arterioscler. Thromb. Vasc. Biol.* **28**, 1304–1310 (2008).
19. Miller, R., Wen, X., Dunford, B., Wang, X. & Suzuki, Y. Cytokine production of $CD8^+$ immune T cells but not of $CD4^+$ T cells from *Toxoplasma gondii*–infected mice is polarized to a type 1 response following stimulation with tachyzoite-infected macrophages. *J. Interferon Cytokine Res.* **26**, 787–792 (2006).
20. Sakaguchi, S. *et al.* $Foxp3^+$ $CD25^+$ $CD4^+$ natural regulatory T cells in dominant self-tolerance and autoimmune disease. *Immunol. Rev.* **212**, 8–27 (2006).
21. Taams, L.S. *et al.* Modulation of monocyte/macrophage function by human $CD4^+CD25^+$ regulatory T cells. *Hum. Immunol.* **66**, 222–230 (2005).
22. Mahajan, D. *et al.* $CD4^+CD25^+$ regulatory T cells protect against injury in an innate murine model of chronic kidney disease. *J. Am. Soc. Nephrol.* **17**, 2731–2741 (2006).

ONLINE METHODS

Mice. We obtained Male C57BL/6J, *ob*/*ob* and *Cd8a*-deficient mice from Charles River Japan or Jackson Laboratories. All mice were housed under a 12-h light-dark cycle and allowed free access to food. To examine the time-course of changes in stromal vascular cell populations in adipose tissue under conditions of diet-induced obesity, we divided C57BL/6 mice into two groups and fed either a standard chow diet (6% fat, Oriental Yeast Company) or a high-fat diet (D12492, 60 Kcal% fat, Research Diets) from the age of 4 weeks.

To examine the effects of CD8 depletion on the initiation and development of adipose inflammation, we started antibody administration before the establishment of DIO. We fed male C57BL/6 mice a high-fat diet for 8 weeks, beginning when they were 4-weeks-old, and we intraperitoneally administered either CD8-specific antibody (3 μg per g body weight, 1 mg ml^{-1} solution, Biolegend) or control rat IgG (Sigma, 1 mg ml^{-1} PBS solution) weekly over the same period. We examined the mice at 12 weeks old (**Fig. 2** and **Supplementary Fig. 7**). We validated depletion of $CD8^+$ T cells by antibody as shown in **Supplementary Figure 11**.

To assess the effects of CD8 depletion on preestablished adipose inflammation in DIO mice, we fed C57BL/6 mice a high-fat diet, beginning when they were 9-weeks-old. Ten weeks later, we randomly assigned the 19-week-old obese mice to two groups and we intraperitoneally administered either CD8-specific antibody (120 μg per mouse) or control IgG three times per week for 2 weeks (total of six administrations). Age-matched lean C57BL/6 mice fed a normal chow diet served as controls. At 21 weeks, we performed oral glucose and insulin tolerance tests and then killed the mice for analysis of their adipose tissue (**Fig. 3** and **Supplementary Fig. 9**).

To assess the effects of CD8-deficient and adoptive transfer of $CD8^+$ T cells on adipose inflammation, we fed *CD8a*$^{-/-}$ mice either normal chow or a high-fat diet for 8 weeks, beginning when they were 6-weeks-old. We intravenously administered either 5×10^6 splenic $CD8^+$ T cells or control PBS weekly over the same period. We examined the *CD8a*$^{-/-}$ mice at 14-weeks-old. We prepared $CD8^+$ splenic T cells from 7-week-old C57BL/6 mice (**Fig. 4** and **Supplementary Fig. 10**). All experiments were approved by the Institutional Committee for Animal Research of The University of Tokyo and strictly adhered to the guidelines for animal experiments of The University of Tokyo.

Isolation of the stromal vascular fraction and flow cytometry. We isolated stromal vascular cells using previously described methods with some modifications. We killed the mice after general anesthesia after systemic heparinization. We removed the epididymal and subcutaneous adipose tissues and then minced it into small pieces (~2 mm). We vigorously agitated the pieces in PBS supplemented with 1 μg ml^{-1} heparin for 30 s to remove any circulating blood cells and then centrifuged the suspension at 1,000*g* for 8 min. We collected floating pieces of adipose tissue and incubated them for 20 min in collagenase solution (2 mg ml^{-1} of collagenase type 2 (Worthington) in Tyrode buffer (containing 137 mM NaCl, 5.4 mM KCl, 1.8 mM $CaCl_2$, 0.5 mM $MgCl_2$, 0.33 mM NaH_2PO_4, 5 mM HEPES and 5 mM glucose)) with gentle stirring. We then centrifuged the digested tissue again at 1,000*g* for 8 min. We resuspended the resultant pellet containing the stromal vascular fraction into PBS and filtered it through a 70-μm mesh. We washed the cells twice with PBS, incubated for 10 min in erythrocyte-lysing buffer (Becton Dickinson) as previously described[3], and we finally resuspended them in PBS supplemented with 3% FBS. We incubated these isolated cells with either labeled monoclonal antibody or isotype control antibody (eBioscience and BD Pharmingen) and analyzed by flow cytometry with a Vantage flow cytometer (Becton Dickinson) and FlowJo (Tree Star, Inc.) software. We used propidium iodide (Invitrogen) to exclude dead cells. We validated flow cytometric identification of M1 ($F4/80^+CD11c^+$) and M2 ($F4/80^+CD11c^-$) macrophages with CD11c markers as described in the **Supplementary Methods** and **Supplementary Figure 12**.

Immunohistochemistry. We stained and visualized whole-mount adipose tissue as previously described[14].

CFSE proliferation assay of $CD8^+$ T cells. We isolated splenic $CD8^+$ T cells from 7-week-old C57BL/6 mice and incubated the isolated $CD3^+$ $CD8^+$ cells with 5 μM CFSE (CellTrace CFSE Cell Proliferation Kit, Invitrogen). After staining, we incubated 2×10^5 cells in DMEM supplemented with 3% FBS for 2 d, with or without 20 mg of minced epididymal white adipose tissue prepared from either 20-week-old lean mice fed a normal chow diet or DIO mice fed a high-fat diet for 16 weeks. We harvested the $CD8^+$ cells and then analyzed them by flow cytometry to examine the proliferation status.

Differentiation of peripheral blood monocytes into macrophages. We isolated peripheral blood monocytes ($CD11b^{high}Gr\text{-}1^-$) from lean 7-week-old C57BL/6 mice. In the lower wells of a 24-well Multiwell Boyden chamber (Becton Dickinson), we cultured 5×10^4 monocytes per well in DMEM supplemented with 3% FBS, with or without 10 mg of minced epididymal adipose tissue prepared from 7-week-old lean mice in the upper wells. Also in the upper wells, we cultured 5×10^4 $CD3^+CD8^+CD4^-$ T cells, which we isolated from epididymal adipose tissues of 20-week-old lean or DIO mice. We incubated the cells for 7 d, after which the cells in the upper wells were collected, stained for CD11b, F4/80 and CD68, and assayed by flow cytometry for the differentiated macrophage fractions ($CD11b^+F4/80^+CD68^+$).

Migration of RAW264.7 and peritoneal macrophages. We isolated $CD8^+$ T cells from blood collected from C57BL/B6J mice after cardiac puncture. We isolated and cultured $CD3^+CD8^+$ cells were in DMEM supplemented with 3% FBS. To activate $CD8^+$ T cells, we cultured the cells with recombinant IL-2 (20 U ml^{-1}; Sigma), Dynabeads CD3/CD28 T Cell Expander (a bead-to-cell ratio of 1:1) and 2-mercaptoethanol (50 μM). After 120 h of culture, we aspirated the culture medium and performed migration assay using Boyden chambers with 8-μm pore inserts (Becton Dickinson). We cultured RAW264.7 and peritoneal macrophages in the upper wells, and we added the conditioned medium to the lower wells. We used fresh DMEM supplemented with 5% FBS as a control. To inhibit MCP-1 activity, we added a neutralizing antibody (5 μg ml^{-1} antibody to MCP-1, clone 2H5, Biolegend) to the conditioned medium.

TNF-α production in macrophages cocultured with $CD8^+$ cells. We isolated $F4/80^+$ $CD11b^+$ macrophages from epididymal adipose tissue from lean 7-week-old C57Bl/B6J mice, and we isolated $CD3^+CD8^+CD4^-$ T cells from epididymal adipose tissue from 20-week-old lean or DIO mice. We then added the adipose macrophages to the upper wells of a Multiwell Boyden chamber (Becton Dickinson) (5×10^4 cells per well), and we added the same number of $CD8^+$ T cells to the lower wells, after which we cultured the cells in DMEM supplemented with 3% FBS for 7 d. We assessed intracellular production of TNF-α by flow cytometry using an intracellular cytokine production detection kit (Cytofix/Cytoperm Fixation/Permeabilization Solution Kit, BD Pharmingen).

Human subjects. We acquired subcutaneous adipose tissue from healthy female donors undergoing liposuction of the abdomen or thighs (after obtaining their consent). We examined expression of *CD8a* in the tissue. We processed samples comprised of 1 g of each specimen by digestion with collagenase and then centrifuged to isolate the stromal vascular fractions. We purified total RNA using Trizol (Invitrogen) and determined relative mRNA levels using real-time PCR. This study was approved by the Ethics Committee of The University of Tokyo Hospital.

Statistical analyses. We expressed the results as means ± s.e.m. We determined the statistical significance of differences between two groups using Student's *t* tests, and we evaluated differences among three groups by analysis of variance followed by *post-hoc* Bonferroni tests. Values of $P < 0.05$ were considered significant.

Supplementary Methods

Animal models

We obtained Male C57BL/6J, ob/ob, and *Cd8a*-deficient mice from Charles River Japan or Jackson Laboratories. All mice were housed under a 12-h light-dark cycle and allowed free access to food.

To examine the time-course of changes in SV cell populations in adipose tissue under conditions of diet-induced obesity, we divided C57BL/6 mice into two groups and fed either a standard chow diet (ND, 6% fat, Oriental Yeast Co., Ltd.) or a high-fat diet (HFD, D12492, 60 Kcal%fat, Research Diets) from the age of 4 weeks. Body weights were significantly higher in diet-induced-obese (DIO) mice fed the high-fat diet than in those fed a control diet (DIO, 40.0±0.9 g; ND, 30.4±0.3 g, n=5 animals, $P < 0.05$) at 21 weeks. Changes in body weight, epididymal fat pad weight, and metabolic phenotypes are shown in Supplementary Fig. 3.

CD8 depletion and adoptive transfer

To establish the $CD8^+$ cell depletion protocol, we first analyzed the effect of the antibody to CD8 (Supplementary Fig. 11) on cell populations in spleen, lymph node, and peripheral blood. Purified rat neutralizing antibody to mouse CD8 (120 μg/mouse, Biolegend) or control rat IgG (Sigma) was intraperitoneally administered to 20-week-old DIO mice. Three days later, we examined lymphocyte and monocyte populations in spleen, lymph node and peripheral blood. We found that the numbers of $CD8^+$ cells were reduced by 70% to 90% in all three tissues from mice administered antibody to CD8. By contrast, CD8-specific antibody treatment did not significantly affect monocyte ($CD11b^{high}Gr\text{-}1^-CD3^-CD94^-$) numbers in peripheral blood, and it

Nature Medicine: doi:10.1038/nm.1964

increased the number of $CD4^+$ cells in the lymph node, though we found no changes in $CD4^+$ cell numbers in the spleen or peripheral blood. These finding demonstrate that administration of CD8-specific antibody was sufficient to efficiently deplete $CD8^+$ cells in mice.

Having confirmed the effectiveness of the CD8-specific antibody, we administered it to mice using three protocols. To examine the effects of CD8 depletion on the initiation and development of adipose inflammation, we started the antibody administration before the establishment of diet-induced obesity. Male C57BL/6 mice were fed a high-fat diet for 8 weeks, beginning when they were 4 weeks old, and we administered intraperitoneally either CD8-specific antibody (3 μg/g body weight) or control IgG weekly over the same period. We examined the mice at 12 weeks old (Fig. 2, and Supplementary Fig. 7).

To assess the effects of CD8 depletion on pre-established adipose inflammation in DIO mice, C57BL/6 mice were fed a high-fat diet, beginning when they were 9 weeks old. Ten weeks later, we randomly assigned the 19-week-old obese mice to two groups and we administered intraperitoneally either CD8-specific antibody (120 μg/mouse) or control IgG three times per week for 2 weeks (total of 6 administrations). Age-matched lean C57BL/6 mice fed a normal chow diet served as controls. At 21 weeks, we performed oral glucose and insulin tolerance tests and then mice were sacrificed for analysis of their adipose tissue (Fig. 3, Supplementary Fig. 9).

To assess the effects of CD8 depletion in ob/ob mice, mice fed a normal diet, and we administered either CD8-specific antibody (120 μg/mouse) or control IgG weekly for 3 weeks, beginning when they were 5 weeks old. We examined them at 8 weeks old (Supplementary Fig. 8).

Nature Medicine: doi:10.1038/nm.1964

To assess the effects of CD8-deficient and adoptive transfer of $CD8^+$ T cells on adipose inflammation, *CD8a*$^{-/-}$ mice were fed either normal chow or a high-fat diet for 8 weeks, beginning when they were 6 weeks old. The mice fed a high-fat diet, and we administered intravenously either 5 x 10^6 splenic $CD8^+$ T cells or control PBS weekly over the same period. We examined the *CD8a*$^{-/-}$ mice at 14 weeks old. We prepared $CD8^+$ splenic T cells from 7-week-old C57BL/6 mice (Fig. 4, Supplementary Fig. 10).

All experiments were approved by the University of Tokyo Ethics Committee for Animal Experiments and strictly adhered to the guidelines for animal experiments of the University of Tokyo.

Glucose and insulin tolerance test

We performed glucose-tolerance (oral, 1 g/kg, after 16 h fasting) and insulin-tolerance (i.p., 0.75-2U/kg: doses shown in Fig. legends, after 3.5 h fasting) tests to assess glucose intolerance and insulin resistance.

Serum cytokine concentration

We examined serum cytokine concentrations using ELISA kits (TNF-α, MCP-1 and IL-6 from R&D, adiponectin from Sekisui-kagaku, insulin and leptin from Morinaga, free fatty acid from Wako).

Flow cytometry

We found that among isolated SV cells, the viable cells were concentrated within the "R1" region (Supplementary Fig. 1), as were the majority of macrophages. Because earlier studies used broader gating to analyze macrophages in the SV fraction [1], we

Nature Medicine: doi:10.1038/nm.1964

compared the conventional wider gating (R2) with the narrower gating used in the present study (R1) in an analysis of the macrophage and lymphocyte fractions (Supplementary Fig. 1). In addition, the increased presence of macrophages was reported in regions that correspond to R3 [2]. Therefore, we also analyzed cells in R3. We found that the $CD11b^+$ $F4/80^+$ macrophage and $CD4^+$ and $CD8^+$ lymphocyte fractions detected using the narrower R1 gating did not significantly differ from those detected using the broader R2 gating. Moreover, the R3 region contained much fewer macrophages and lymphocytes than R1. Indeed, there were no significant differences among the cell-type fractions within R1, R2 and R2+R3 (Supplementary Table 1, Two-way ANOVA). Based on these findings, we analyzed the cell populations gated to R1.

The antibodies used were specific to CD3 (145-2C11, BDpharmingen), CD4 (RM4-5, BDpharmingen), CD8a (53-6.7, BDpharmingen, or KT15 Abcam), CD11c (HL-3, eBioscience), CD25 (PC62, BDpharmingen), CD94 (18d3, eBioscience), CD206 (MR5D3, Serotec), F4/80 (BM8, Caltag), Foxp3 (FJK-16s, eBioscience), GR-1 (RB6-8C5), TNFα (MP6-XT22, BDpharmingen), and IL-10 (JES5-16E3, BDpharmingen).

We analyzed intracellular cytokine production using a Cytofix/Cytoperm Fixation/Permeabilization Solution Kit (BD Pharmingen). We examined TCR Vβ repertoire using a Mouse Vβ TCR Screening Panel kit (BDpharmingen).

To differentiate M1 from M2 macrophages in the SV fraction, we analyzed expression of M1 and M2 markers, and intracellular cytokine production [3-5] in $F4/80^+$ $CD11c^+$ and $F4/80^+$ $CD11c^-$ cells, which reportedly exhibit the M1 and M2 phenotypes, respectively, in adipose tissue [6] (Supplementary Fig. 12). We found that the majority

(82-86%) of F4/80^{+}CD11c^{+} cells were positive for TNFα and negative for CD206 (mannose receptor) and IL-10, while the majority (65-75%) of F4/80^{+}CD11c^{-} cells were negative for TNFα production and positive for CD206 and IL-10 expression. These data indicate that F4/80^{+}CD11c^{+} and F4/80^{+}CD11c^{-} macrophages largely exhibit the phenotypes of M1 and M2 macrophages, respectively. Based on these results we used a combination of F4/80 and CD11c to differentiate M1 and M2 macrophages.

Immunohistochemistry

For immunohistochemical analyses, mice were sacrificed by cervical dislocation, after which the epididymal and femoral subcutaneous fat pads were removed using sterile technique and minced into small pieces (~2-3 mm) using a scalpel. We washed the tissue pieces, fixed them in 4% formaldehyde for 45 min and permeabilized with 1% Triton X-100 (CalBiochem) for 10 min. The specimens were then blocked with 1% bovine serum albumin and incubated first with a primary antibody [specific to F4/80 (Caltag, BM-8), CD4 (BioLegend, RM4-5), or CD8 (Abcam, 53-6.7); 1:100 dilution] for 12 h and then with Alexa Fluor 488-conjugated secondary antibody (Molecular Probes) for 1 h. The tissues were counterstained for 1 h with 5 μM BODIPY 558/568 C12 (Molecular Probes) to visualize adipocytes and with 40 μM Hoechst 33342 (Molecular Probes) to visualize nuclei. We stained vasculature with *Griffonia simplicifolia* IB_4 isolectin conjugated with AlexaFluor 488 (Molecular Probes, 20μg/ml) for 1 h. We excited the tissue samples using three laser lines (405 nm, 488 nm and 568 nm), and collected the emission through appropriate narrow band-pass filters. We collected 2- to 5-μm-thick stacks of images at 0.5 μm intervals along the optical axis. Each image was produced from an average of 8 video frames using IpLab software v3.6

Nature Medicine: doi:10.1038/nm.1964

(Scanalytics), after which the acquired images were processed using VoxBlast software (Vaytek) to produce a surface-rendered 3-dimensional model.

Quantitative analysis of adipocytes, stromal cells and crown-like structures

We determined adipocyte diameters using IpLab software. Images of 5 randomly selected low-power fields were acquired from four animals in each group, after which the diameters of 50 cells in each field were measured by an observer blinded to the conditions. To quantify the numbers of crown-like structures and stromal cells, we obtained 20 images of cells stained with BODIPY and Hoechst plus antibody to F4/80, antibody to CD8 or isolectin from 4 animals in each group. We determined the numbers of crown-like structures (defined as an adipocyte with a disrupted plasma membrane surrounded by accumulated cells and/or engulfing macrophages) and positively stained cells using IpLab software by an observer blinded to the conditions.

Real-time quantitative PCR

For real-time PCR, we homogenized entire adipose tissue in Trizol (Invitrogen), after which total RNA was purified from the homogenates. We determined relative mRNA levels using a Superarray kit (Superarray) according to the manufacture's instructions.

Human Subjects

After obtaining informed consent using an institutional review board-approved protocol, we acquired subcutaneous adipose tissue from healthy female donors undergoing liposuction of the abdomen or thighs [7]. We examined expression of *CD8a* in the tissue. We processed samples comprised of 1 g of each specimen by digestion with collagenase

Nature Medicine: doi:10.1038/nm.1964

and then centrifuged to isolate the SV fractions. We purified total RNA using Trizol (Invitrogen), and determined relative mRNA levels using real-time PCR. This study was approved by the ethics committee of the University of Tokyo Hospital.

CFSE proliferation assay of $CD8^+$ T cells

We isolated splenic $CD8^+$ T cells from 7-week-old C57BL/6 mice. We performed cell sorting using a Vantage cell sorter (Becton Dickinson) after staining with FITC-CD3 and PE-Cy7-CD8 antibody. We used propidium iodide to exclude dead cells. We incubated the isolated $CD3^+$ $CD8^+$ cells with 5μM CFSE (CellTrace CFSE Cell Proliferation Kit, Invitrogen) for 15 min. After staining, we incubated 2 x 10^5 cells in Dulbecco's modified Eagle's medium (DMEM) supplemented with 3% FBS for two days, with or without 20 mg of minced epididymal white adipose tissue prepared from either 20-week-old lean mice fed a normal chow diet or DIO mice fed a high-fat diet for 16 weeks. We harvested the $CD8^+$ cells and then analyzed by flow cytometry to examine the proliferation status.

Differentiation of peripheral blood monocytes into macrophages

We isolated peripheral blood monocytes ($CD11b^{high}$ $Gr\text{-}1^-$) from lean 7-week-old C57BL/6 mice. In the lower wells of a 24-well Multiwell Boyden chamber (BD), we cultured 5 x 10^4 monocytes per well in DMEM supplemented with 3% FBS, with or without 10 mg of minced epididymal adipose tissue prepared from 7-week-old lean mice in the upper wells. Also in the upper wells, we cultured 5 x 10^4 $CD3^+CD8^+CD4^-$ T cells, which were isolated from epididymal adipose tissues of 20-week-old lean or DIO mice. We incubated the cells for 7 days, after which the cells in the upper wells were

Nature Medicine: doi:10.1038/nm.1964

harvested, stained for CD11b, F4/80 and CD68, and assayed by flow cytometry for the differentiated macrophage fractions ($CD11b^+$ $F4/80^+$ $CD68^+$).

Migration of RAW264.7 and peritoneal macrophages

We isolated $CD8^+$ T cells from blood collected from C57Bl/B6J mice following cardiac puncture. We isolated peritoneal macrophages as previously described [8]. We performed cell sorting using a Vantage cell sorter after staining with FITC-CD3-antibody and PE-Cy7-CD8-antibody. $CD3^+CD8^+$ cells were isolated and cultured in DMEM supplemented with 3% fetal bovine serum (FBS). To activate $CD8^+$ T cells, we cultured the cells with recombinant IL-2 (20 U/ml; Sigma), Dynabeads CD3/CD28 T Cell Expander (a bead-to-cell ratio of 1:1) and 2-mercaptoethanol (50 μM). After 120 h of culture, we aspirated the culture medium and filtered. The T cell expander beads were removed by a magnet. We performed migration assay using Boyden chambers with 8-μm pore inserts (BD). We cultured RAW264.7 and peritoneal macrophages in upper wells, and we added the conditioned medium to the lower wells. We used fresh DMEM supplemented with 5% FBS as a control. Cells that migrated to the lower surface of the insert were stained with FM1-43 (Molecular Probes) and Hoechst 33342 (Molecular Probes), and then counted under a confocal microscope by observers blinded to the conditions. To inhibit MCP-1 activity, we added a neutralizing antibody (5μg/ml, antibody to MCP-1, clone 2H5, Biolegend) to the conditioned medium. We determined cytokine concentrations in conditioned medium using the microbeads array method by Charles River Laboratories.

TNF-α production in macrophages cocultured with $CD8^+$ cells

We isolated $F4/80^+$ $CD11b^+$ macrophages from epididymal adipose tissue from lean

Nature Medicine: doi:10.1038/nm.1964

7-week-old C57Bl/B6J mice, and $CD3^+CD8^+CD4^-$ T cells were isolated from epididymal adipose tissue from 20-week-old lean or DIO mice. The adipose macrophages were then added to the upper wells of a Multiwell Boyden chamber (BD) (5×10^4 cells/well), and the same number of $CD8^+$ T cells were added to the lower wells, after which the cells were cultured in DMEM supplemented with 3% FBS for 7 days. We assessed intracellular production of TNF-α by flow cytometry using an intracellular cytokine production detection kit (Cytofix/Cytoperm Fixation/Permeabilization Solution Kit, BD Pharmingen).

Statistics

We expressed the results as means ± S.E.M. The statistical significance of differences between two groups were determined using Student's t-tests; differences among three groups were evaluated using ANOVA followed by post hoc Bonferroni tests. We examined the correlation using Pearson correlation coefficient test. Values of $P < 0.05$ were considered significant.

References

1. Traktuev, D.O., *et al.* A population of multipotent CD34-positive adipose stromal cells share pericyte and mesenchymal surface markers, reside in a periendothelial location, and stabilize endothelial networks. *Circ Res* **102**, 77-85 (2008).
2. Brake, D.K., Smith, E.O., Mersmann, H., Smith, C.W. & Robker, R.L. ICAM-1 expression in adipose tissue: effects of diet-induced obesity in mice. *Am J Physiol Cell Physiol* **291**, C1232-1239 (2006).
3. Bourlier, V., *et al.* Remodeling phenotype of human subcutaneous adipose tissue macrophages. *Circulation* **117**, 806-815 (2008).
4. Gordon, S. & Taylor, P.R. Monocyte and macrophage heterogeneity. *Nat Rev Immunol* **5**, 953-964 (2005).

5. Sica, A., Schioppa, T., Mantovani, A. & Allavena, P. Tumour-associated macrophages are a distinct M2 polarised population promoting tumour progression: potential targets of anti-cancer therapy. *Eur J Cancer* **42**, 717-727 (2006).
6. Lumeng, C.N., Bodzin, J.L. & Saltiel, A.R. Obesity induces a phenotypic switch in adipose tissue macrophage polarization. *J Clin Invest* **117**, 175-184 (2007).
7. Suga, H.*, et al.* Numerical measurement of viable and nonviable adipocytes and other cellular components in aspirated fat tissue. *Plast Reconstr Surg* **122**, 103-114 (2008).
8. Coleman, D.L., Bartiss, A.H., Sukhatme, V.P., Liu, J. & Rupprecht, H.D. Lipopolysaccharide induces Egr-1 mRNA and protein in murine peritoneal macrophages. *J Immunol* **149**, 3045-3051 (1992).

Nature Medicine: doi:10.1038/nm.1964

Supplementary Table1 Calculated %cells per total live cells in each gating

%cells/Live cells	gate R1	gate R2	gate R2+R3
Macrophage (F4/80+ CD11b+)	10.1%±1.4%	12.4%±1.6%	13.7%±1.6%
CD8 (CD3+ CD8+ CD4-)	8.0%±1.4%	9.0%±1.3%	9.9%±1.6%
CD4 (CD3+ CD8- CD4+)	3.0%±0.3%	3.7%±0.5%	4.0%±0.5%

The macrophage and lymphocyte fractions per total viable cells within each gating region are shown. There were no significant differences among the cell type fractions in the R1, R2 and R2+R3 regions (Two-way ANOVA).

Nature Medicine: doi:10.1038/nm.1964

Supplementary Figures

Supplementary Figure 1

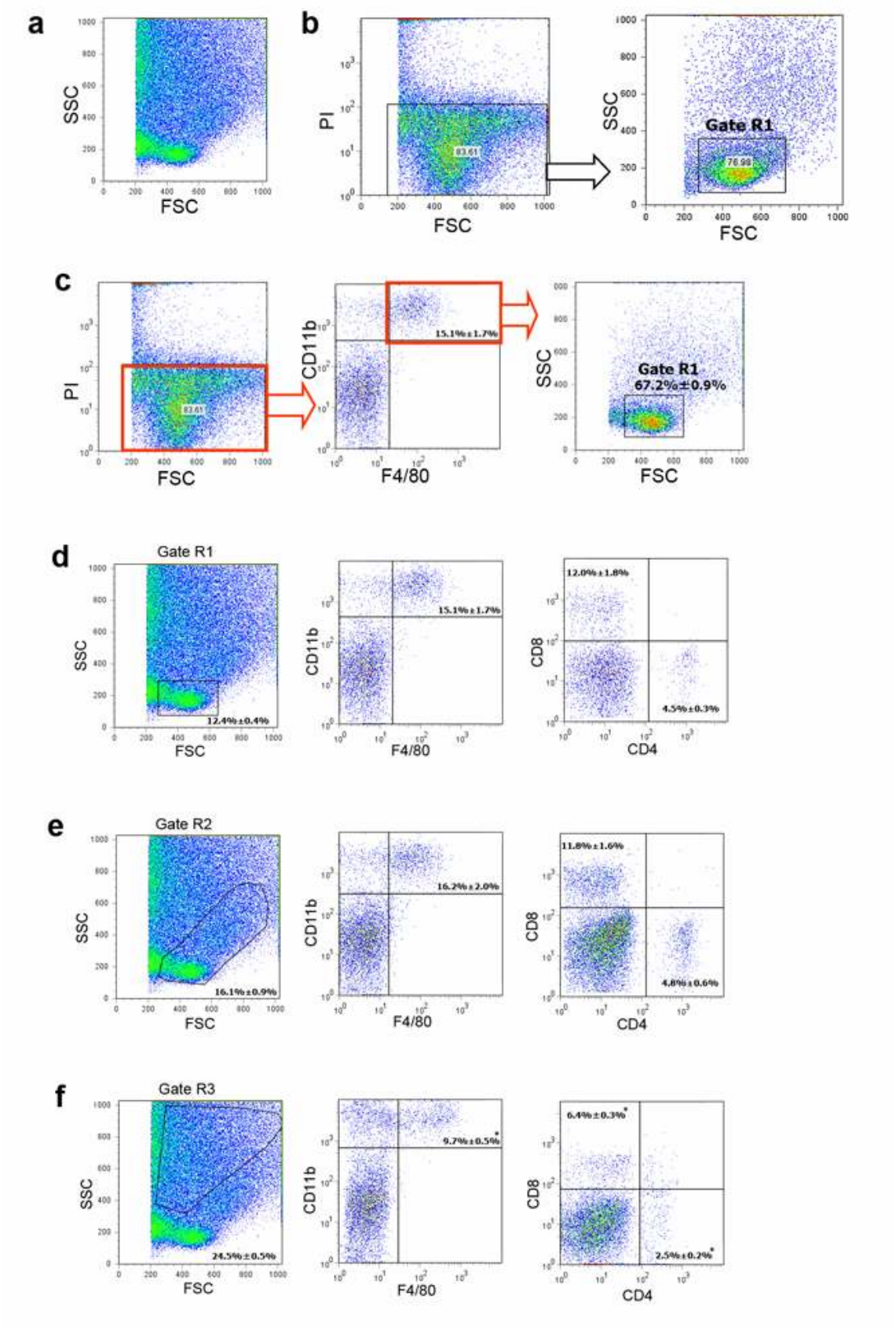

Nature Medicine: doi:10.1038/nm.1964

Gating of immune cell populations in SVF

(**a**) FSC/SSC plot of total isolated SVF cells from 20-week-old DIO mice. On the FSC/SSC plot is a region in which most of the viable cells were located. We set a gate (R1) for this cell population. (**b**) FSC/SSC plot of viable cells (PI^-). Note that the viable cells were concentrated within R1. (**c**) Distribution of viable macrophages (PI^- $F4/80^+$ $CD11b^+$) on the FSC/SSC plot. Note that the majority (~67%) of viable macrophages were also located within R1. (**d-f**) Gating of immune cell populations in SVF. Earlier studies used broader gating to analyze macrophages in the SV fraction (R2) [1]. In addition, the presence of macrophages was reported in the R3 region (**f**) [2]. In the present study, therefore, we analyzed viable cells within both narrow (**d**, R1) and wider (**e**, R2) and R3 (**f**) gating regions. The results show that choosing R1 or R2 did not significantly affect the macrophage and lymphocyte fractions. Within R3 there were much fewer macrophages and lymphocytes than in R1. Consequently, the macrophage and $CD8^+$ and $CD4^+$ cell fractions did not significantly differ between R1, R2 and R2+R3 (see Supplementary Table 1). n=5 animals in each group. (*$P < 0.05$ vs. R1 in d-f).

Nature Medicine: doi:10.1038/nm.1964

Supplementary Figure 2

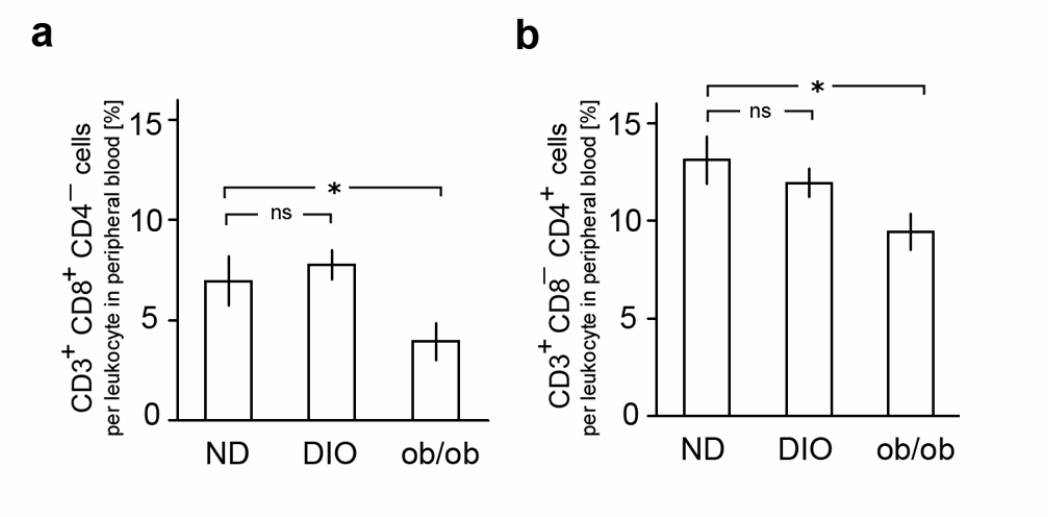

CD8$^+$ and CD4$^+$ T cells in peripheral leukocytes

$CD3^+CD8^+CD4^-$ (**a**) and $CD3^+CD8^-CD4^+$ (**b**) T cell fractions were analyzed by flow cytometry using peripheral leukocytes from 20-week-old control lean (ND) mice, diet-induced obese (DIO) mice and ob/ob mice (n=5 animals in each group; *$P < 0.05$).

Nature Medicine: doi:10.1038/nm.1964

Supplementary Figure 3

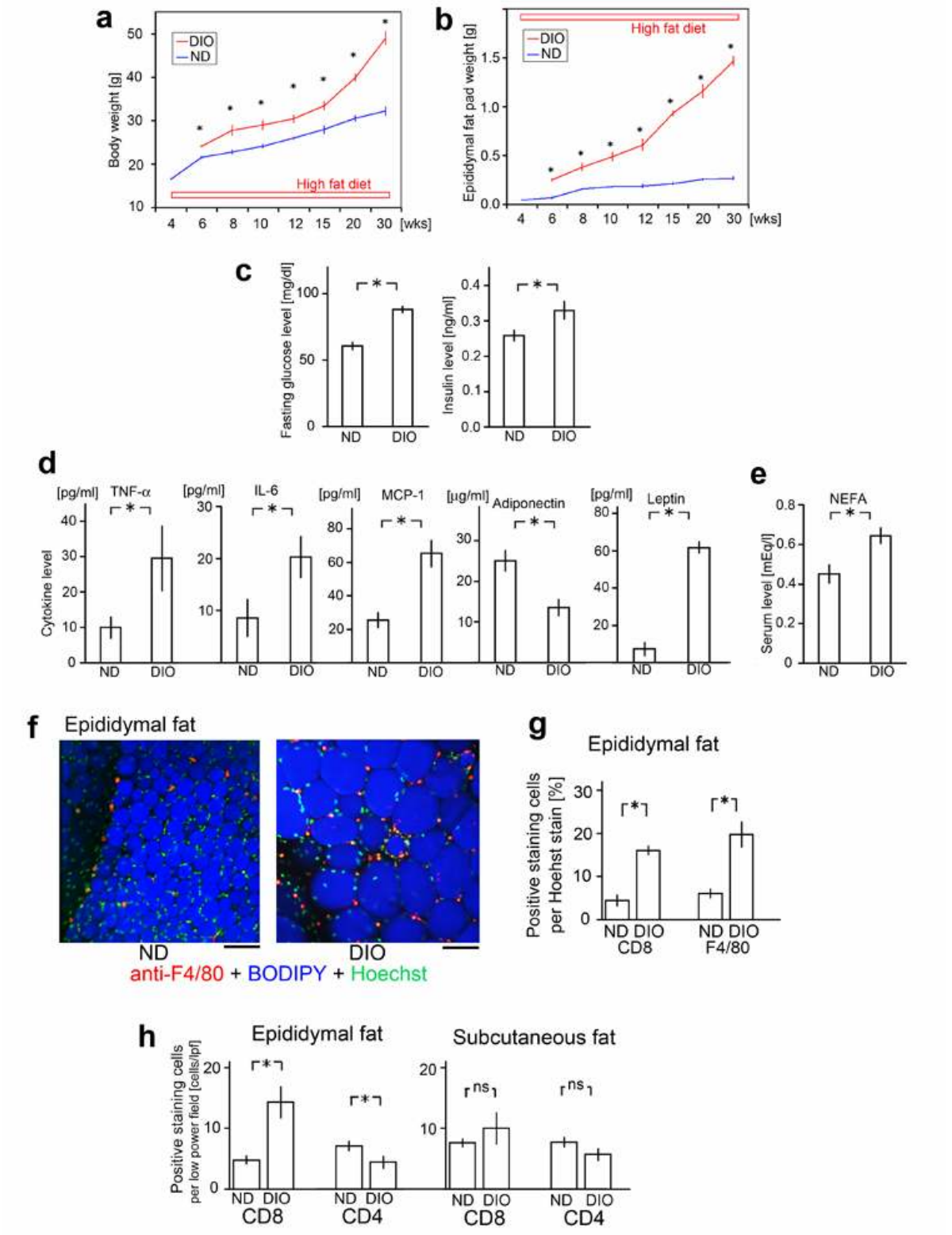

Nature Medicine: doi:10.1038/nm.1964

Metabolic phenotypes and adipose tissue hitochemistry in ND and DIO mice

The body (**a**) and epididymal fat pad (**b**) weight changes in wild-type mice fed a normal diet (ND, blue) or a high-fat diet (DIO, red), as shown in Fig. 1d-g. The high-fat diet was started at 4 weeks of age, as indicated (red boxes). (**c-e**) Metabolic profiles of 20-week-old ND and DIO mice fasted for 16 h (n=5 animals in each group; $*P < 0.05$). Fasting glucose levels (**c**) and (**d,e**) serum levels of insulin, TNF-α, IL-6, MCP-1, adiponectin, leptin, and nonesterified fatty acids (NEFA) (n=5 animals under 16 h fasting in each group, $*P < 0.05$). (**f**) Immunohistochemical identification of macrophages (F4/80, red) in epididymal adipose tissue from ND and DIO mice. Adipocytes were counterstained with BODIPY (blue), and the nuclei were stained with Hoechst (green). Scale bar, 100 μm. (**g,h**) Quantification of $CD8^+$ and $CD4^+$ T cells in epididymal and femoral subcutaneous adipose tissue from ND and DIO mice. The numbers of $CD8^+$, $CD4^+$ cells and macrophages are expressed as positive staining cells per number of $Hoechst^+$ nuclei or low power field images (20 low-power fields from 5 animals in each group). Note that the macrophage and $CD8^+$ T cell fractions are similar to those detected by flow cytometry (Fig. 1). ($*P < 0.05$; ns, not significant).

Nature Medicine: doi:10.1038/nm.1964

Supplementary Figure 4

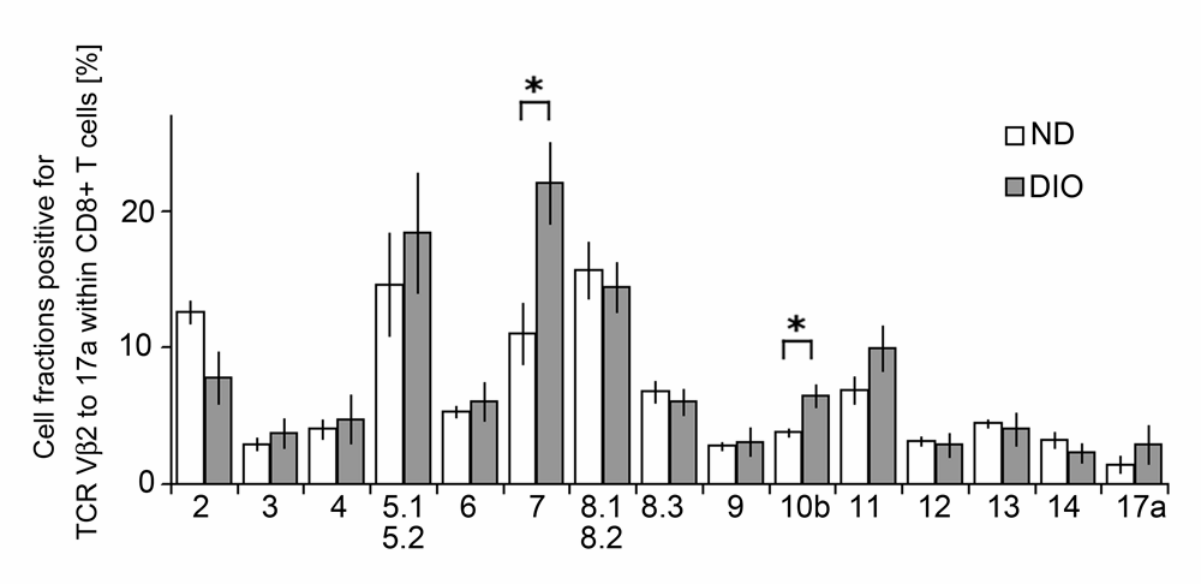

Flow cytometric analysis of the T cell receptor repertoire in $CD8^+$ T cells in adipose tissue

Flow cytometric analysis of the T cell receptor (TCR) Vβ repertoire in $CD8^+$ cells in the SV fraction from lean mice fed a normal chow diet (ND, white bars) and diet-induced obese mice fed a high-fat diet for 16 weeks (DIO, gray bars). Cell fractions positive for TCR Vβ2 to 17a within $CD8^+$ cells are shown (n=5 animals in each group; $*P < 0.05$). All mice were 20 weeks old.

Nature Medicine: doi:10.1038/nm.1964

Supplementary Figure 5

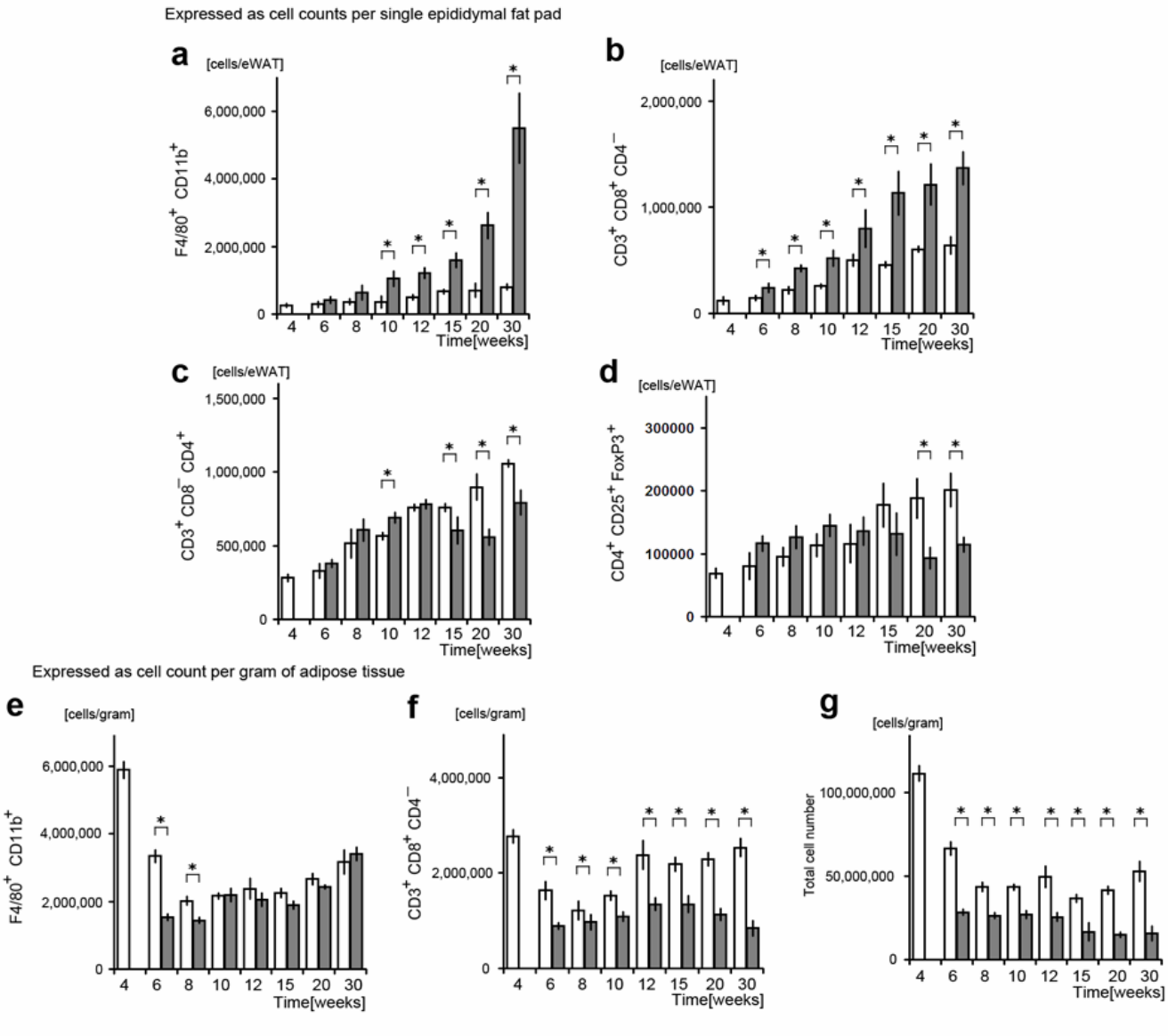

Time-course of changes in the cell populations expressed per epididymal fat pad or gram of epididymal fat tissue

Flow cytometric analysis of the SV fraction from the epididymal fat pads of control mice fed a normal chow diet (white bars) or mice fed a high-fat diet, beginning when the mice were 4 weeks old (gray bars), as shown in Figure 1d-g. (a-d) The numbers are expressed as cells per epididymal fat pad (eWAT). Numbers of macrophages (a, $F4/80^{+}CD11b^{+}$), $CD8^{+}$ T cells (b, $CD3^{+}CD8^{+}CD4^{-}$), $CD4^{+}$ T cells (c, $CD3^{+}CD8^{-}CD4^{+}$) and regulatory T cells (d, $CD4^{+}CD25^{+}Foxp3^{+}$) were determined during the course of DIO development. Note that the

Nature Medicine: doi:10.1038/nm.1964

increase in $CD8^+$ cells preceded the macrophage infiltration when expressed as numbers of cells per fat pad. (e-g) Cell numbers expressed as cells per gram of epididymal fat. Numbers of macrophages (e, $F4/80^+CD11b^+$), $CD8^+$ T cells (f, $CD3^+CD8^+CD4^-$), and total isolated viable cells (g) were determined. Note that the total cell numbers per gram were notably smaller in obese animals than lean animals because of the rapid hypertrophy of adipocytes, and consequently, the numbers of $CD8^+$ T cells are fewer in a gram of obese adipose than lean adipose. n=5 animals in each group. (*$P < 0.05$).

Nature Medicine: doi:10.1038/nm.1964

Supplementary Figure 6

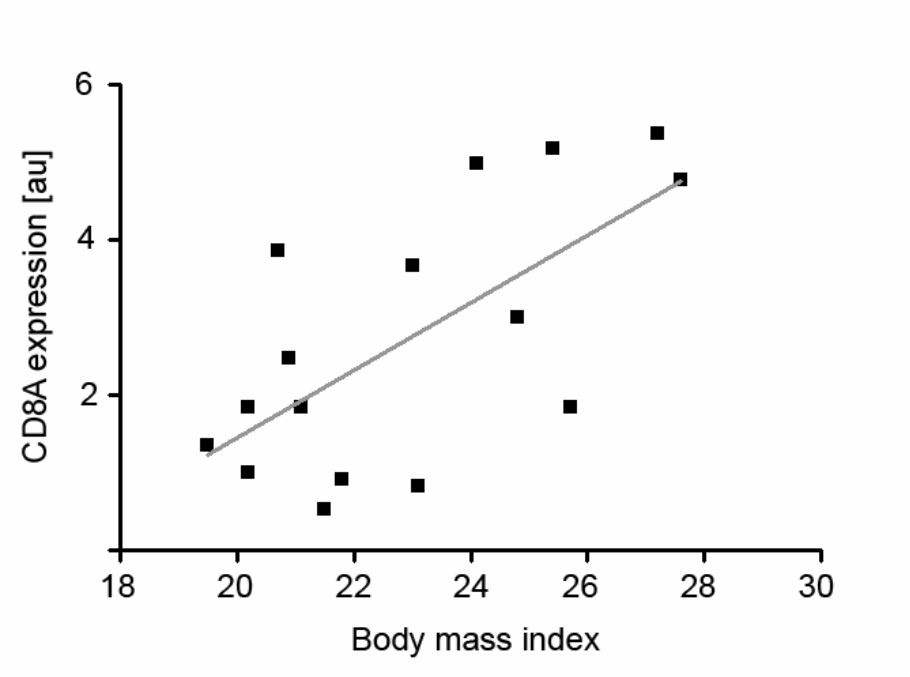

***CD8A* expression in human subcutaneous fat tissues**

Levels of *CD8A* expression in the SV fraction from subcutaneous fat pad surgically obtained from human subjects were analyzed. There is a positive correlation between the *CD8A* level and body mass index (BMI) (R=0.66 by Pearson correlation coefficient test, n=16 subjects, $P < 0.05$).

Nature Medicine: doi:10.1038/nm.1964

Supplementary Figure 7

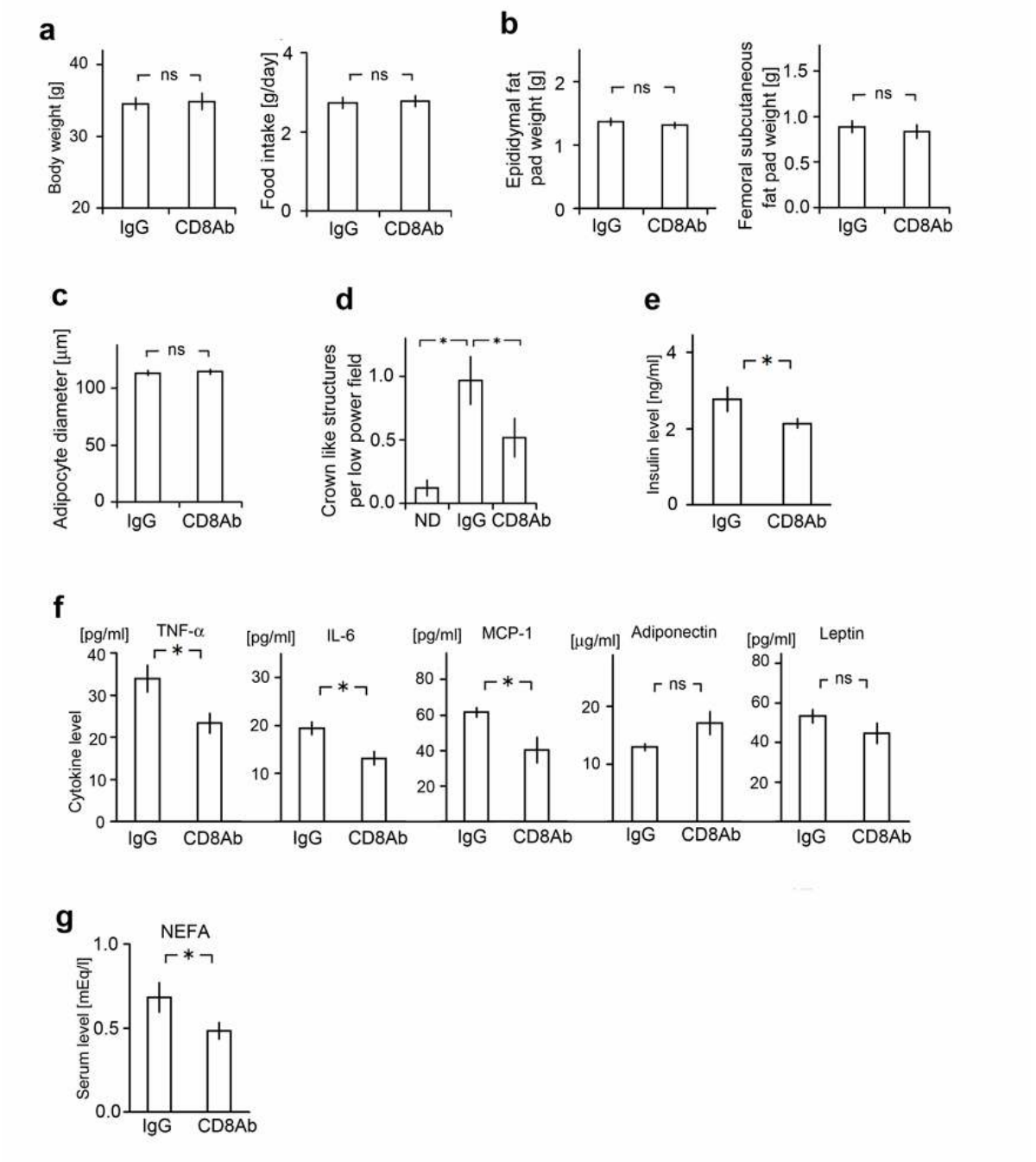

Effects of the long-term CD8 depletion on the metabolic profiles of mice fed a high-fat diet

C57BL/6 mice were administered either antibody to CD8 (CD8 Ab) or control IgG (IgG) weekly for 8 weeks, beginning when they were 4 weeks old. They were also fed a high-fat diet over the same period, as shown in Figure 2. All mice were examined when they were 12 weeks old. (**a, b, c**) Body weight, daily food intake, epididymal fat pad weight, femoral

Nature Medicine: doi:10.1038/nm.1964

subcutaneous fat pad weight, and mean adipocyte diameter in the epididymal fat pads are shown (n=8 animals in each group). Mean adipocyte diameters were calculated from a total of 200 adipocytes randomly selected from 25 low-power fields (n=8 animals in each group; ns, not significant). (**d**) Numbers of crown-like structures (white arrows in Fig. 2b) in adipose tissue (n=20 low-power fields in each group, $*P < 0.05$). Twelve-week-old lean mice fed a normal chow diet (ND) served as a control. (**e, f, g**) Serum levels of insulin, TNF-α, IL-6, MCP-1, adiponectin, leptin, and nonesterified fatty acids (NEFA) in mice treated with IgG or CD8 Ab (n=8 animals under ad-libitum feeding in each group). ($*P < 0.05$; ns, not significant).

Nature Medicine: doi:10.1038/nm.1964

Supplementary Figure 8

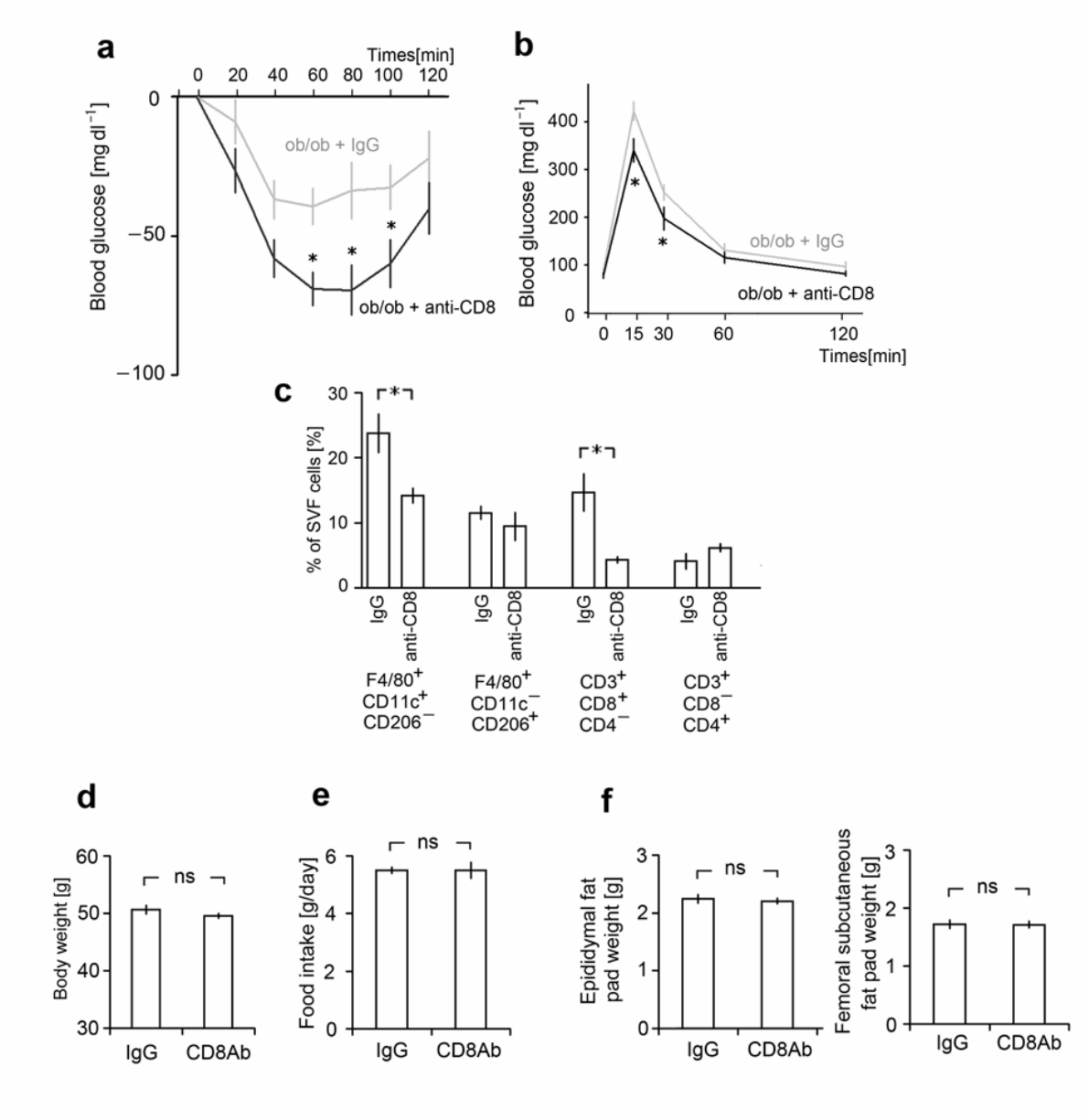

Effects of CD8$^+$ cell depletion in ob/ob mice

ob/ob mice fed a normal diet were randomly assigned to two groups and administered either antibody to CD8 (CD8 Ab, 120 μg/mouse) or control IgG (IgG) weekly for 3 weeks, beginning when the were 5 weeks old. They were then examined at 8 weeks old. (a, b) Results of insulin-tolerance (**a**, 2 U/kg insulin) and oral glucose-tolerance (**b**, 1 g/kg glucose) tests in mice administered anti-CD8 Ab (ob/ob + anti-CD8, black lines) or control IgG (ob/ob + IgG, gray lines) (n=6 animals in each group, *$P < 0.05$). (**c**) Flow cytometric analysis of M1 macrophages (F4/80$^+$CD11c$^+$CD206$^-$), M2 macrophages (F4/80$^+$CD11c$^-$CD206$^+$), CD8$^+$ T

Nature Medicine: doi:10.1038/nm.1964

cells, and $CD4^+$ T cells in SV fractions (n=5 animals in each group, $*P < 0.05$). Body weight (**d**), daily food intake (**e**), epididymal fat pad weight (**f**), and femoral subcutaneous fat pad weight in ob/ob mice treated with IgG and anti-CD8 Ab (n=6 animals in each group; ns, not significant).

Nature Medicine: doi:10.1038/nm.1964

Supplementary Figure 9

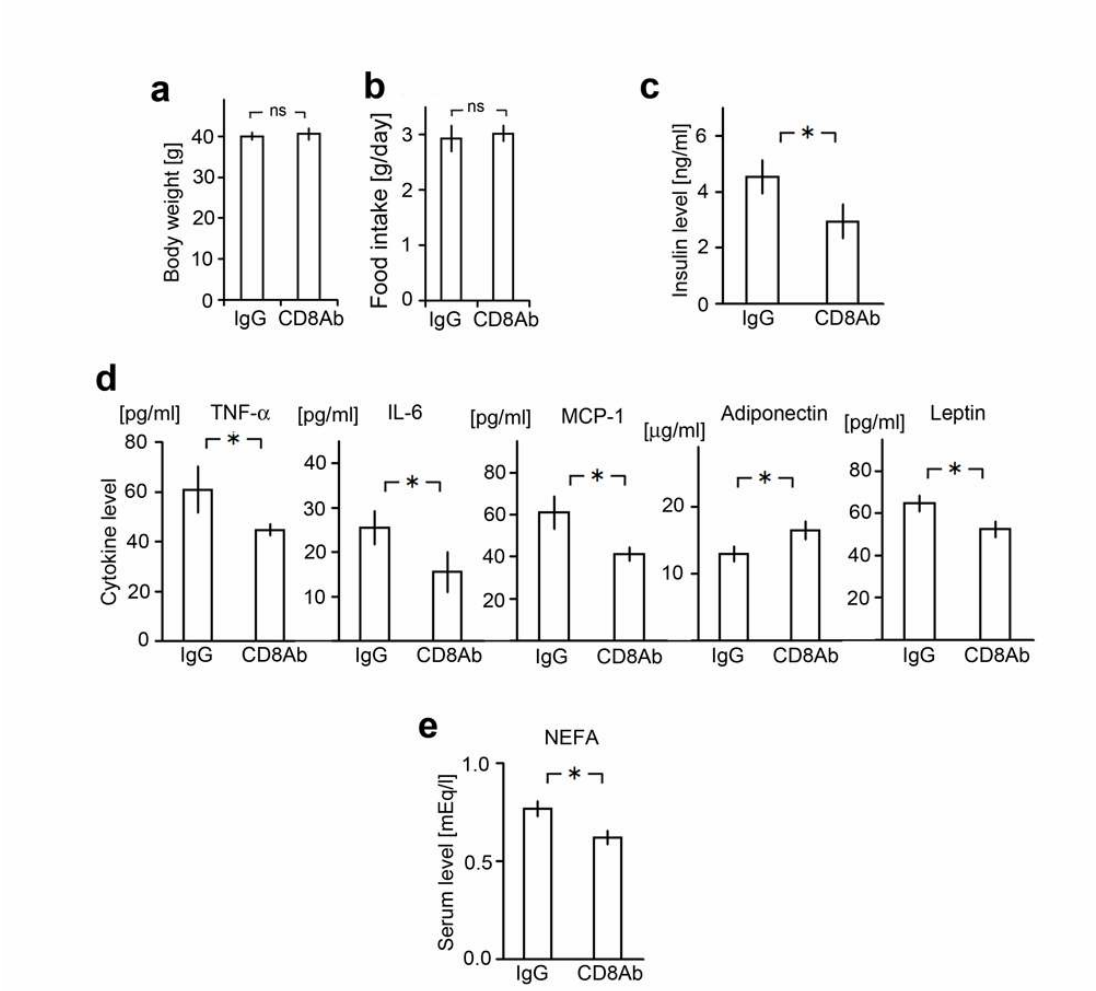

Effects of CD8-specific antibody treatment on metabolic profiles in pre-established DIO mice

C57BL/6 mice were fed a high-fat diet, beginning when they were 9 weeks old. Beginning at 19 weeks, they were administered either antibody to CD8 (CD8 Ab) or control IgG (IgG) for 2 weeks, as in Figure 3. Lean mice fed a normal chow served as controls (ND). All mice were examined when they were 21 weeks old. (**a, b**) Body weight (**a**) and daily food intake (**b**) of DIO + CD8 and DIO + IgG mice (n=10 animals in each group; ns, not significant). (**c, d, e**) Serum levels of insulin, TNF-α, IL-6, MCP-1, adiponectin, leptin, and nonesterified fatty acids (NEFA) in mice treated with IgG or anti-CD8 Ab (n=10 animals fed ad-libitum in each group, $*P < 0.05$).

Nature Medicine: doi:10.1038/nm.1964

Supplementary Figure 10

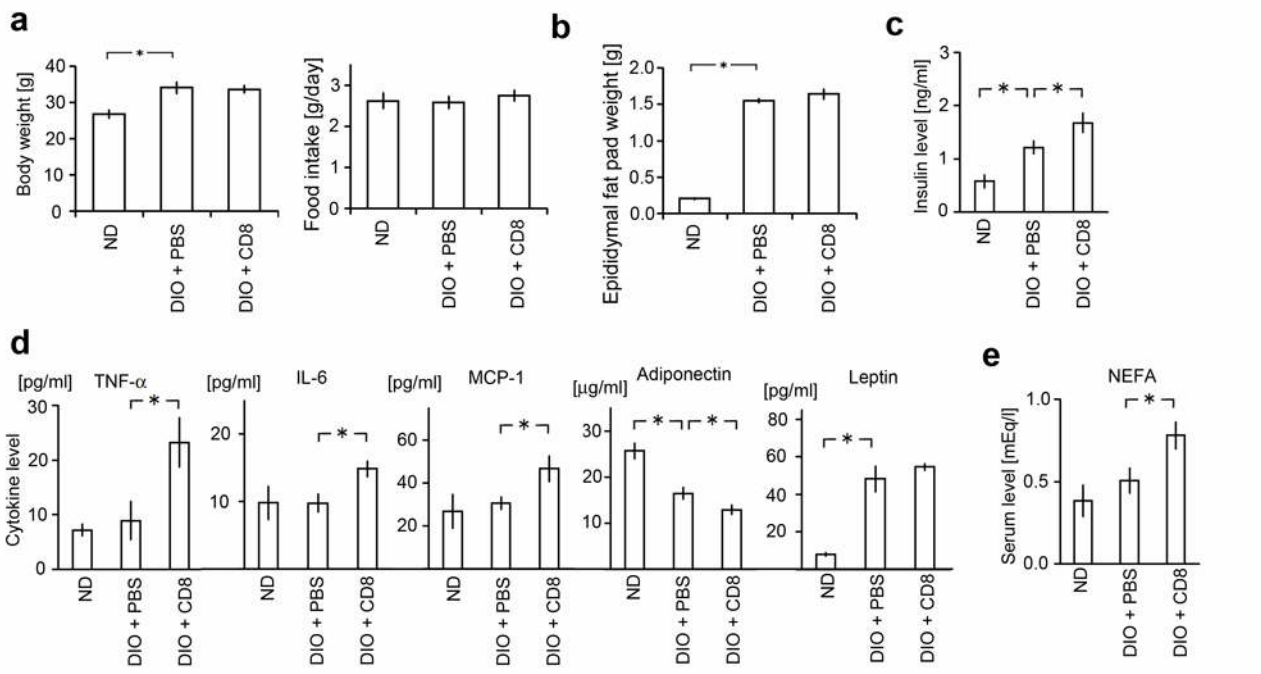

Effects on metabolic profiles of adoptive transfer of CD8$^+$ T cells to *Cd8a*-deficient mice

Cd8a$^{-/-}$ mice were fed either normal chow (ND) or a high-fat diet (DIO) for 8 weeks, beginning when they were 6 weeks old. Splenic CD8$^+$ T cells (5 x 10^6) isolated from lean control mice (DIO + CD8) or PBS (DIO + PBS) were intravenously administered to the DIO mice weekly over the same period, and the mice were examined at 14 weeks old. (**a, b**) Body weight, daily food intake, and epididymal fat pad weight in ND, DIO + PBS and DIO + CD8 mice (n=6 animals in each group, **P* < 0.05). (**c, d, e**) Serum levels of insulin, TNF-α, IL-6, MCP-1, adiponectin, leptin, and nonesterified fatty acids (NEFA) in ND, DIO + PBS and DIO + CD8 mice (n=6 animals under ad-libitum feeding in each group, **P* < 0.05).

Nature Medicine: doi:10.1038/nm.1964

Supplementary Figure 11

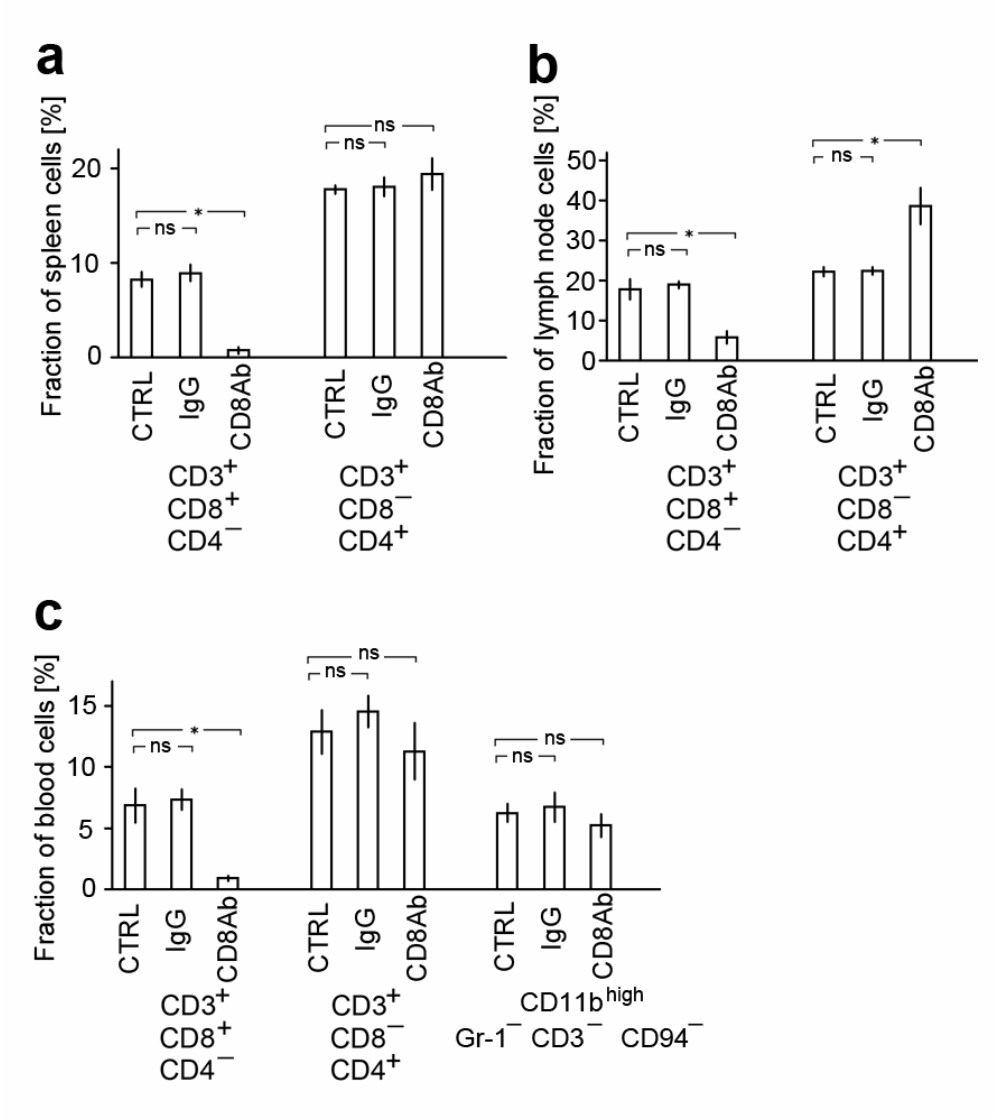

Validation of CD8 depletion by antibody to CD8 treatment

Neutralizing antibody to CD8 (CD8 Ab, 120 μg/mouse) or control rat IgG (IgG) was intraperitoneally administered to 20-week-old DIO mice 3 days before examination. Untreated DIO mice served as a control (CTRL). Lymphocyte and monocyte populations were examined in the spleen (**a**), lymph node (**b**), and peripheral blood (**c**). CD8 Ab treatment reduced the numbers of $CD8^+$ cells by 70% to 90% in all three tissues. By contrast, monocyte ($CD11b^{high}Gr\text{-}1^-CD3^-CD94^-$) numbers in peripheral blood were not significantly altered by CD8 Ab treatment.

Nature Medicine: doi:10.1038/nm.1964

Supplementary Figure 12

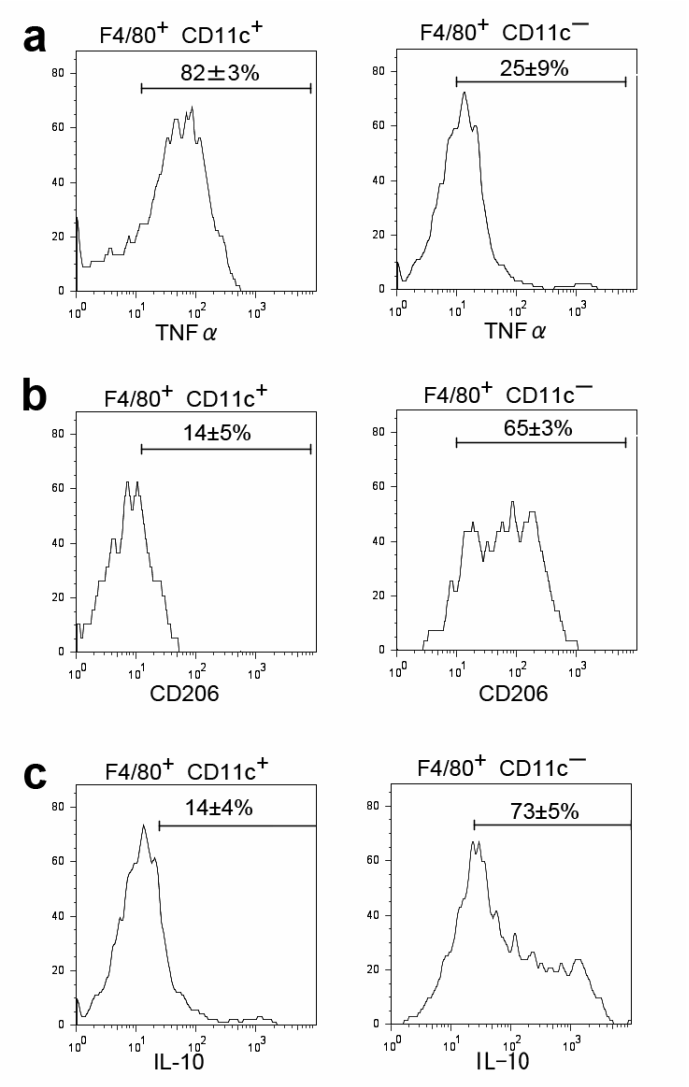

CD11c as a marker of M1 and M2 macrophage differentiation

To validate CD11c as a marker for discriminating the M1 and M2 subsets of macrophages in adipose tissue, expression levels of TNFα (**a**), CD206 (**b**) and IL-10 (**c**) were examined in the F4/80$^+$ CD11c$^+$ and F4/80$^+$ CD11c$^-$ cell populations in the SV fraction from 20-week-old DIO mice. We found that the majority of F4/80$^+$ CD11c$^+$ cells were positive for TNFα and negative for CD206 and IL-10, while F4/80$^+$ CD11c$^-$ cells were largely negative for TNFα and positive for CD206 and IL-10. Positive cells were determined by isotype-matched control antibody staining. These data indicate that F4/80$^+$ CD11c$^+$ and F4/80$^+$ CD11c$^-$ macrophages respectively exhibit the M1 and M2 phenotypes [3-5].

Nature Medicine: doi:10.1038/nm.1964

References

1. Traktuev, D.O.*, et al.* A population of multipotent CD34-positive adipose stromal cells share pericyte and mesenchymal surface markers, reside in a periendothelial location, and stabilize endothelial networks. *Circ Res* **102**, 77-85 (2008).
2. Brake, D.K., Smith, E.O., Mersmann, H., Smith, C.W. & Robker, R.L. ICAM-1 expression in adipose tissue: effects of diet-induced obesity in mice. *Am J Physiol Cell Physiol* **291**, C1232-1239 (2006).
3. Gordon, S. & Taylor, P.R. Monocyte and macrophage heterogeneity. *Nat Rev Immunol* **5**, 953-964 (2005).
4. Lumeng, C.N., Bodzin, J.L. & Saltiel, A.R. Obesity induces a phenotypic switch in adipose tissue macrophage polarization. *J Clin Invest* **117**, 175-184 (2007).
5. Bourlier, V.*, et al.* Remodeling phenotype of human subcutaneous adipose tissue macrophages. *Circulation* **117**, 806-815 (2008).

Nature Medicine: doi:10.1038/nm.1964